Future prospects for exploring present day anomalies in flavour physics measurements with Belle II and LHCb

J. Albrecht[a] F. U. Bernlochner[b,c] M. Kenzie[d] S. Reichert[a] D. M. Straub[e] A. Tully[d]

[a]*Fakultät Physik, Technische Universität Dortmund, Dortmund, Germany*

[b]*Physikalisches Institut der Rheinischen Friedrich-Wilhelms-Universität, Bonn, Germany*

[c]*Institut für Experimentelle Kernphysik, Karlsruhe Institute of Technology, Karlsruhe, Germany*

[d]*Cavendish Laboratory, University of Cambridge, Cambridge, UK*

[e]*Excellence Cluster Universe, Garching, Germany*

E-mail: matthew.kenzie@cern.ch, stefanie.reichert@cern.ch

ABSTRACT: A range of flavour physics observables show tensions with their corresponding Standard Model expectations: measurements of leptonic flavour-changing neutral current processes and ratios of semi-leptonic branching fractions involving different generations of leptons show deviations of the order of four standard deviations. If confirmed, either would be an intriguing sign of new physics. In this manuscript, we analyse the current experimental situation of such processes and estimate how the future flavour factory Belle II and the future running periods of LHCb and its upgrade will be able to influence the present tensions with the standard model expectations. In addition, the present day and future sensitivity of tree-level CKM parameters, which offer complementary tests of the Standard Model, are explored. Three benchmark points in time are chosen for a direct comparison of the estimated sensitivity between the experiments. A high complementarity between the future sensitivity achieved by the Belle II and LHCb experiments is observed due to the different strengths and weaknesses of both experiments. We estimate that all of the anomalies considered here will be either confirmed or ruled out by both experiments independently with very high significance by the end of data-taking at Belle II and the LHCb upgrade.

Contents

1 Introduction

The study of precision observables at the B factory experiments BaBar [1] and Belle [2], as well as at LHCb [3] have gained renewed attention recently: several measurements challenge the lepton flavour universality (LFU) assumed in the Standard Model (SM) and show apparent deviations in the electroweak couplings between the three generations of leptons, see e.g. Refs. [4, 5] for two recent reviews. In this manuscript, the present day and future sensitivities of these signatures at the upcoming flavour factory Belle II [6] and the planned running periods of LHCb and its upgrade [7] are discussed. In addition, the expected development of the precision of observables relevant to measure the Cabibbo-Kobayashi-Maskawa (CKM) quark mixing matrix [8, 9] is detailed. Precision CKM measurements offer a potent way to test the SM by over-constraining the predicted unitarity of the CKM matrix. Specifically, the following observables have been studied:

1. The CKM parameters $|V_{ub}|$, $|V_{cb}|$, and γ: These observables are often considered as benchmarks for the SM because they can be determined exclusively by tree-level processes. Any disagreement between tree and loop determinations of the CKM parameters would be clear evidence of new physics (NP) participating in either the tree or loop diagrams (or both). Furthermore, measurements of $|V_{ub}|$ and $|V_{cb}|$ using different methods show a long-standing tension, diminishing the full potential of this test.

2. The ratio of tree-level semi-tauonic decays compared to the $\ell = e, \mu$ light lepton final states: This ratio has been measured in $b \to c\tau\nu_\tau$ decays with D an D^* final states [10–16] reconstructed using either the leptonic or hadronic τ decay final states. LFU violation is expected in the presence of new phenomena contributing to these processes such as leptoquarks or new charged currents. The latest experimental measurements of these ratios show a deviation from the SM expectation of about 4σ, where σ is the standard deviation.

3. Flavour-changing neutral current decays: Decays involving $b \to s$ transitions are loop- and CKM-suppressed in the SM and thus exceptionally sensitive to NP. A large number of measurements has been performed, first by the B factories, then at the Large Hadron Collider (LHC), in particular by the LHCb experiment. While no conclusive evidence for physics beyond the SM has emerged, numerous deviations from SM predictions have been observed in the flavour sector. Discrepancies in tests of lepton flavour universality at the level of $2 - 3\sigma$ have been measured in the ratios between $B \to K^{(*)}\mu^+\mu^-$ and $B \to K^{(*)}e^+e^-$ branching fractions [17, 18] and further tensions between the SM predictions and measurements of $b \to s\ell^+\ell^-$ transitions [19–24] point towards a deficit in branching fractions involving decays with muons in the final state.

For the projections of the future Belle II and LHCb sensitivity, published measurements are extrapolated to the expected integrated luminosities. In the case of LHCb, the $b\bar{b}$-production cross-sections are assumed to scale linearly with centre-of-mass energy, $\sqrt{s}$, as indicated by the existing measurements [25, 26]. The trigger efficiencies of the LHCb upgrade are assumed to improve due to the implementation of a full software trigger according to Ref. [27]. Some future extrapolations for LHCb are also taken from Ref. [7]. In the case of Belle II many extrapolations are also taken from Ref. [28], which provides a full overview of the Belle II physics program and potential.

An overview of the expected Belle II and LHCb data taking periods is given in Figure 1. Using these periods, three 'milestone' points are chosen to provide estimated sensitivities in the years 2020, 2024 and 2030. They are summarised in Table 1 and defined as follows: The Belle experiment has recorded $0.7\,\mathrm{ab}^{-1}$ at the $\Upsilon(4S)$ centre-of-mass energy throughout its running in the years 1999 – 2010 and the LHCb experiment has recorded $3\,\mathrm{fb}^{-1}$ in Run 1 (2010 – 2012) of the LHC. The Belle II experiment plans to record collisions at the $\Upsilon(4S)$ centre-of-mass energy in 2018 and will have accumulated a dataset of about $5\,\mathrm{ab}^{-1}$ by 2020, which corresponds to about four times the dataset of the existing B factories. This dataset can be compared to the end of the Run 2 data set of LHCb of $8\,\mathrm{fb}^{-1}$, which will be recorded by the end of 2018. These two datasets define the first 'milestone'. By mid 2024 Belle II will have accumulated its full envisioned $\Upsilon(4S)$ dataset of about $50\,\mathrm{ab}^{-1}$. At this point in time the LHCb phase 1 upgrade plans to have recorded a dataset of $22\,\mathrm{fb}^{-1}$ using collisions from Run 3 (2021 – 2023) of the LHC. This defines the second 'milestone'. As of now, no concrete plans exist for a possible Belle II upgrade, thus no assumptions beyond 2024 are made for Belle II. The LHCb phase 1 upgrade plans to collect a total dataset of $50\,\mathrm{fb}^{-1}$ by 2029 using collisions from Run 4 (2026 – 2029) of the LHC, marking the third 'milestone'

scenario. The timelines of the future data taking of the Belle II and LHCb experiments are taken from Ref. [28] and from the LHC roadmap [29].

The LHCb experiment has recently expressed its interest to continue running after the phase 1 upgrade [30]. This phase 2 upgrade is suggested to run until the end of the funded LHC Run, 2035, and will collect a total dataset of $300\,\text{fb}^{-1}$. The phase 2 upgrade of LHCb is not further discussed in this document. The Belle II experiment plans also to record datasets beyond the $\Upsilon(4S)$ centre-of-mass energy, which will allow for studies of higher mass states, for example the B_s-meson. As these plans are not detailed at this point in time, we will not further discuss them in this document.

Table 1: The luminosity scenarios considered along with the estimated number of $b\bar{b}$-pairs produced inside the acceptance of the experiments are given. The LHCb cross sections are taken from Ref. [25] assuming a linear increase in $b\bar{b}$-production cross section with LHC beam energy. For Belle II only $e^+e^- \to \Upsilon(4S) \to B\bar{B}$ data sets are estimated.

			'Milestone I'	'Milestone II'	'Milestone III'
year		2012	2020	2024	2030
LHCb	$\mathcal{L}\,[\,\text{fb}^{-1}\,]$	3	8	22	50
	$n(b\bar{b})$	0.3×10^{12}	1.1×10^{12}	37×10^{12}	87×10^{12}
	$\sqrt{s}$	$7/8\,\text{TeV}$	$13\,\text{TeV}$	$14\,\text{TeV}$	$14\,\text{TeV}$
Belle (II)	$\mathcal{L}\,[\,\text{ab}^{-1}\,]$	0.7	5	50	-
	$n(B\bar{B})$	0.1×10^{10}	0.54×10^{10}	5.4×10^{10}	-
	$\sqrt{s}$	$10.58\,\text{GeV}$	$10.58\,\text{GeV}$	$10.58\,\text{GeV}$	-

The remainder of this manuscript is structured as follows: In Section 2, tests of the CKM structure of the SM are detailed. Section 3 discusses the test of LFU in tree level semi-leptonic decays. Section 4 focuses on flavour-changing neutral current decays based on $b \to s$ transitions, including loop-level tests of LFU and a study of the impact of the future experiments on the knowledge of the Wilson coefficients. The manuscript concludes with Section 5 which summarises the main findings.

2 Measurements of tree-level CKM parameters

The flavour structure, and consequent phenomena of CP violation, in the quark sector of the SM are completely described by the CKM quark mixing matrix [8, 9]. A common representation of the CKM constraints is portrayed in the Argand plane as the so-called unitarity triangle, which has a single unknown apex $(\bar{\rho}, \bar{\eta})$. This point can be uniquely determined using the length of the side opposite the well-measured angle β, which is proportional to the ratio $|V_{ub}|/|V_{cb}|$, and the relatively poorly-known angle γ. Both of these can be determined from tree-level decays. Under the SM hypothesis, the apex determined using γ and $|V_{ub}|/|V_{cb}|$ should be the same as that determined from β and $\Delta m_d/\Delta m_s$, which are determined from loop decays. Given the latter are considerably better measured than the former, precision determinations of γ, $|V_{ub}|$ and $|V_{cb}|$ are important tests of the CKM
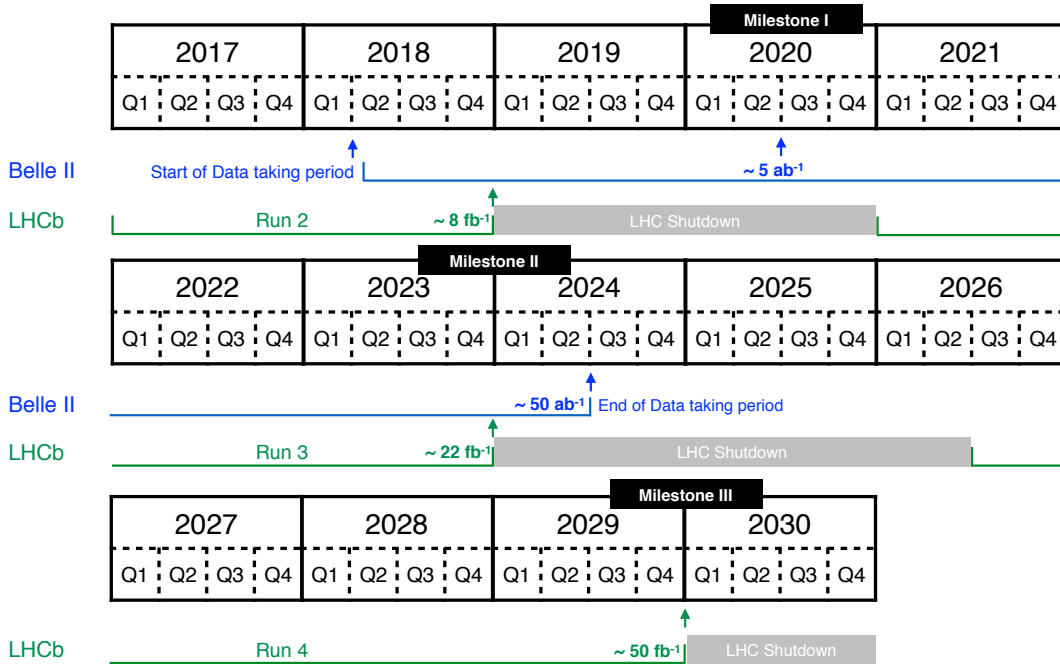
Figure 1: An overview of the expected Belle II and LHCb timelines along with their estimated integrated luminosities at each milestone. The scenarios compared in this manuscript are shown in bold. For more details of the expected luminosities and number of produced $b\bar{b}$-pairs at each milestone see Table 1. The LHCb Phase-I-Upgrade [27] is currently scheduled for the duration of the LHC shutdown between 2019 – 2020. The LHCb experiment has recently expressed its interest to continue running past the Phase-I-Upgrade until the end of the funded LHC Run in 2035 [30].

structure of the SM. It has been shown that the current experimental constraints on the Wilson coefficients governing decays of the form $b \to u_1 \bar{u}_2 d_1$, where $u_{1,2}$ are up-type quarks and d_1 is a down-type quark, can still easily allow for tree-level new physics effects of order 10% [31]. Effects of this size can cause shifts in the tree-level determination of γ of up to $4°$. Thus, comparison between the point in $(\bar{\rho}, \bar{\eta})$ space determined using γ and $|V_{ub}|/|V_{cb}|$ with that found using $\sin(2\beta)$ and $\Delta m_d/\Delta m_s$ is a cornerstone of the flavour physics program at both LHCb and Belle II, where any discrepancies will be of huge importance.

Sensitivity to $|V_{ub}|$ and $|V_{cb}|$ arises from the semileptonic transitions $b \to u\ell\bar{\nu}_\ell$ and $b \to c\ell\bar{\nu}_\ell$ respectively. This can be achieved with two different analysis techniques; using either inclusive or exclusive final states. Exclusive measurements use specific decay modes which proceed via a $b \to u$ or $b \to c$ transition, for example $B \to \pi\ell\nu$ [32] or $B \to D\ell\nu$ [33], to determine $|V_{ub}|$ and $|V_{cb}|$ respectively.[i] These require experimental extraction of the differential decay rate along with theoretical input parameterising the form factor. Inclusive measurements use the sum of all possible decays of the type $b \to u\ell\bar{\nu}_\ell$ and $b \to c\ell\bar{\nu}_\ell$, for

---

[i]Charge conjugation is implied throughout.

$|V_{ub}|$ and $|V_{cb}|$ respectively. These are experimentally more challenging due to considerable background contamination which can only be removed by restriction to a particular region of the available phase space. Extraction of $|V_{ub}|$ and $|V_{cb}|$ in the hadronic environment of the LHC is extremely challenging, if not impossible, using the channels described above. Instead, LHCb has pioneered a new approach in which the ratio $|V_{ub}|/|V_{cb}|$ is extracted using baryonic decays of $\Lambda_b^0 \to p\mu^-\nu$ relative to $\Lambda_b^0 \to \Lambda_c^+\mu^-\nu$ [34]. This is equivalent to an exclusive determination and requires input from lattice QCD of the relevant form factors.

Historically, there has been something of a puzzle surrounding these measurements because of a long standing discrepancy between inclusive and exclusive approaches, shown in Fig. 2 (numbers sourced from Ref. [35]). Resolving and understanding these discrepancies, whether physically motivated by new physics or due to theoretical or experimental oversights, is an important goal for upcoming flavour physics experiments. In this section the impact of upcoming data from the Belle II [6] and LHCb experiments [7] is estimated, where the current world averages from Ref. [35] are used for the central values. Estimates for the future projections of the uncertainties for Belle II come from Ref. [28], whilst for the $|V_{ub}|/|V_{cb}|$ ratio measurement from LHCb the experimental uncertainty is reduced by the square-root of the expected yield increase which arises from the increased luminosity, collision energy and trigger improvement. It has been conservatively assumed that this eventually hits the limit of the dominant systematic uncertainty (knowledge of the $\Lambda_b^0 \to pK^+\pi^-$ branching fraction). Furthermore, we assume modest improvement to the uncertainty arising from lattice QCD. The values used are shown in Table 2 and the projection of the future impact shown in Fig. 3, using the `GammaCombo` package [36]. Figure 3 demonstrates that the largest improvement for inclusive measurements comes from the first milestone of Belle II, with relatively little further impact from the second milestone. Conversely, for exclusive measurements at Belle II the big improvement, especially for $|V_{cb}|$, comes from the large increase in the sample size of Belle II at the second milestone. For the LHCb baryonic measurement the biggest improvement comes from the increase in luminosity for the first milestone but is then halted as the measurement hits the systematic limit originating from knowledge of the $\Lambda_b^0 \to pK^+\pi^-$ branching fraction. Figure 4 shows the compatibilty of the current measurements and future projections with the SM in the difference between inclusive and exclusive measurements. This demonstrates that, if the current central values stay the same, the discrepancy will be well beyond 5σ. An additional figure in Appendix A, Fig. 9, shows the compatibilty, at 1σ, between the current world averages for inclusive and exclusive determinations of $|V_{ub}|$ and $|V_{cb}|$, alongside the projected uncertainties at 1σ, 3σ and 5σ when the Belle II and LHCb experiments have finished running, assuming the central values stay the same.

One possible explanation for the discrepancy between inclusive and exclusive measurements of $|V_{ub}|$ and $|V_{cb}|$ has been to introduce a new current which couples only to right-handed fermions [37]. This explanation is probed by exploring the dependence of $|V_{ub}|$ as a left-handed only coupling, $|V_{ub}^L|$, on the size of the assumed right-handed coupling, ϵ_R. Tensions and prospects for these related measurements have been explored using the values shown in Table 3, which are obtained for Belle II measurements from [28], and using the same projections from LHCb for $\Lambda_b^0 \to p\mu^-\nu$ as in Table 2, with an additional source of

uncertainty arising from the $|V_{cb}|$ normalisation term, which is dominated by knowledge of the $\Lambda_b^0 \to \Lambda_c^+ \mu^- \nu$ branching fraction. The projections are shown in Fig. 5 in which the central values are taken from the existing measurements (as listed in Table 3). This shows that the most dramatic improvement comes at the first milestone for the inclusive, $B \to \pi \ell \nu$ and $\Lambda_b^0 \to p \mu^- \nu$ measurements, whilst the $B^- \to \tau^- \bar{\nu}$ improvement continues towards milestone III. Appendix A has an additional figure, Fig. 11, in which the central values which have been shifted to the SM expectation from Ref. [38] with $\epsilon_R = 0$ and $|V_{ub}| = (3.72 \pm 0.06) \times 10^{-3}$.

It is worth noting that some recent developments regarding the parametrisation of the form factor for the exclusive determination of $|V_{cb}|$ from $B \to D^* \ell \bar{\nu}_\ell$ decays [39, 40] have found a value much more consistent with that of the inclusive analyses. The measurements presented in this document, taken directly from Ref. [35], use the Caprini-Lellouch-Neubert (CLN) parametrisation [41], which hitherto has been the one applied by the experimental collaborations. The present level of experimental accuracy calls for a more careful treatment of the associated theoretical uncertainties [42]. An alternative parametrisation from Boyd, Grinstein and Lebed (BGL) [43] results in values closer to the inclusive determination, depending on the particular parameters used. Clearly, deeper understanding of both the experimental and theoretical approaches is necessary to resolve these discrepancies [44].

Precision measurements of $|V_{ub}|$ and $|V_{cb}|$ can be combined with measurements of the CKM angle γ to determine a uniquely tree-level measurement of the CKM parameters $(\bar{\rho}, \bar{\eta})$, under the SM hypothesis. This is a good probe for new physics when compared to measurements of $\sin(2\beta)$, Δm_d and Δm_s which determine the same point from loop processes. The direct determination of the CKM angle γ predominantly uses decays of the form $B^- \to D^0 K^-$ where the ratio between the favoured $b \to c$ and supressed $b \to u$ transitions goes like $r e^{i(\delta - \gamma)}$, where r and δ are unknown hadronic parameters. A comprehensive review on the determination of γ can be found in Refs. [45, 46]. Prospects for improved determinations of the CKM angle γ from both Belle II and LHCb are considerable. By the end of milestone I (II) Belle II expect to determine γ with 6° (1.5°) precision [28]. LHCb expect to determine γ at the level of 4° (milestone I), 1.5° (milestone II) and < 1° (milestone III) [7].

The projections for exclusive and inclusive determination of $|V_{ub}|$ and $|V_{cb}|$, overlaid with those for direct determination of CKM angle γ, are shown in Fig. 6. This is overlaid with the current world average using all contraints on $(\bar{\rho}, \bar{\eta})$ from the CKMfitter collaboration [38]. It it noticeable that already there is some tension between $|V_{ub}|/|V_{cb}|$ measurements and the CKM fit. An additional figure in Appendix A, Fig. 12, shows the same plot with the current experimental constraints on $\sin(2\beta)$ and $\Delta m_d/\Delta m_s$, from Ref. [35], additionally overlaid.

## 3 Lepton flavour universality in trees

A key test of LFU is measuring the ratio of branching fractions of decays that differ only by the lepton content of the final state. Measurements of this type are represented by

Table 2: Values used for the projections of future $|V_{ub}|$ and $|V_{cb}|$ measurements

Measurement	Current World Average ($\times 10^{-3}$) (Ref. [35])	Current Uncertainty (Ref. [35])	Projected Uncertainty				
			Belle II		LHCb		
			$5\,\mathrm{ab}^{-1}$	$50\,\mathrm{ab}^{-1}$	$8\,\mathrm{fb}^{-1}$	$22\,\mathrm{fb}^{-1}$	$50\,\mathrm{fb}^{-1}$
$|V_{ub}|$ inclusive	4.49 ± 0.23	5.1%	3.4%	3.0%	-	-	-
$|V_{ub}|$ exclusive	3.72 ± 0.19	5.1%	2.5%	2.1%	-	-	-
$|V_{cb}|$ inclusive	42.2 ± 0.8	1.9%	1.3%	1.2%	-	-	-
$|V_{cb}|$ exclusive	39.2 ± 0.7	1.8%	1.6%	1.1%	-	-	-
$|V_{ub}|/|V_{cb}|$	83.0 ± 5.7	6.9%	-	-	3.4%	3.0%	2.3%

Table 3: Values used for the projections of future limits on right-handed currents

Measurement	Current World Average ($\times 10^{-3}$) (Ref. [35])	Current Uncertainty (Ref. [35])	Projected Uncertainty				
			Belle II		LHCb		
			$5\,\mathrm{ab}^{-1}$	$50\,\mathrm{ab}^{-1}$	$8\,\mathrm{fb}^{-1}$	$22\,\mathrm{fb}^{-1}$	$50\,\mathrm{fb}^{-1}$
Inclusive	4.49 ± 0.23	5.1%	3.4%	3.0%	-	-	-
$B^- \to \tau^- \overline{\nu}$	4.2 ± 0.4	9.5%	4.7%	2.2%	-	-	-
$B^0 \to \pi^- \ell^+ \nu$	3.72 ± 0.16	4.3%	2.0%	1.5%	-	-	-
$\Lambda_b^0 \to p\mu^- \nu$	3.27 ± 0.23	6.9%	-	-	3.9%	3.5%	2.9%
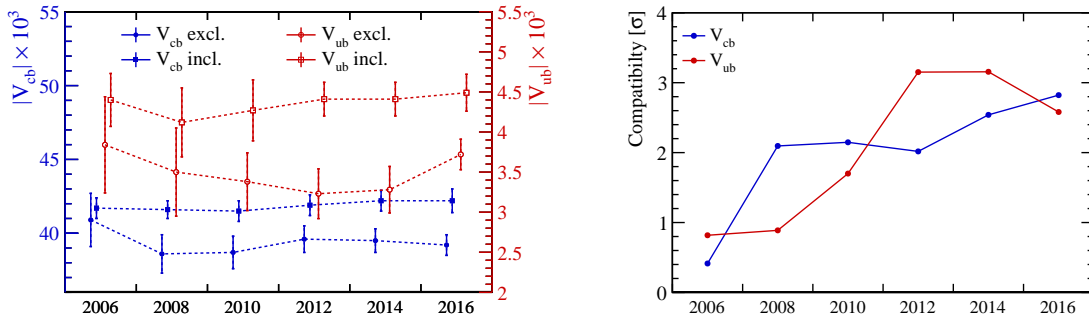
(a) Progression of inclusive (square points) and exclusive (circular points) measurements of $|V_{ub}|$ (red) and $|V_{cb}|$ (blue)

(b) Compatibility, in standard deviations (σ), between inclusive and exclusive measurements of $|V_{ub}|$ (red) and $|V_{cb}|$ (blue)

Figure 2: Historical progression of inclusive and exclusive measurements of $|V_{ub}|$ and $|V_{cb}|$ from Ref. [35].

the observable $R(X)$, which denotes the ratio of branching fractions of $B \to X\ell\nu$ (or $B \to X\ell^+\ell^-$ in the next section) decays, for two choices of ℓ, where ℓ can be e, μ or τ.

A large class of SM extensions contain new interactions that couple preferentially to the third generation of quarks and leptons, such as models involving Higgs-like charged scalars or W' bosons. Ratios involving tree-level $b \to c\tau\nu$ transitions are particularly sensitive to these NP scenarios. Two of these observables, $R(D)$ and $R(D^*)$, are defined as the ratio
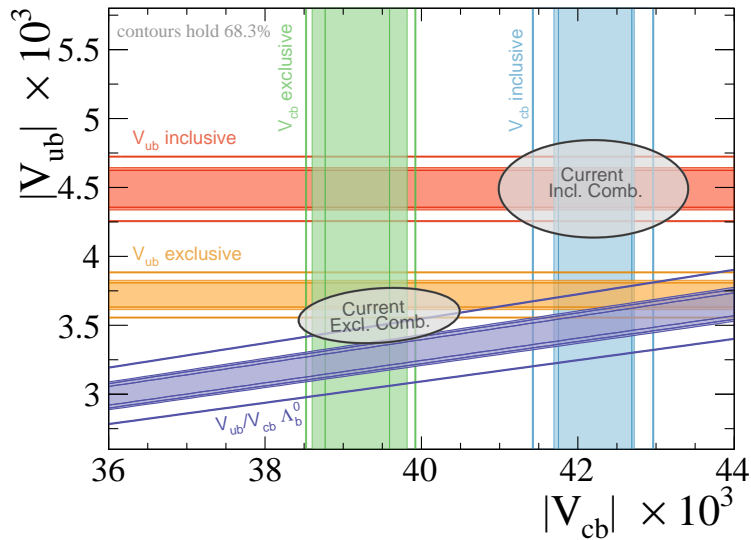
Figure 3: Prospects of the future sensitivity for various inclusive and exclusive measurements of $|V_{ub}|$ and $|V_{cb}|$ with the current world averages from Ref. [35] (not filled) and the future projections at milestones I, II and III (filled). The current inclusive and exclusive combinations are shown as the gray filled areas.
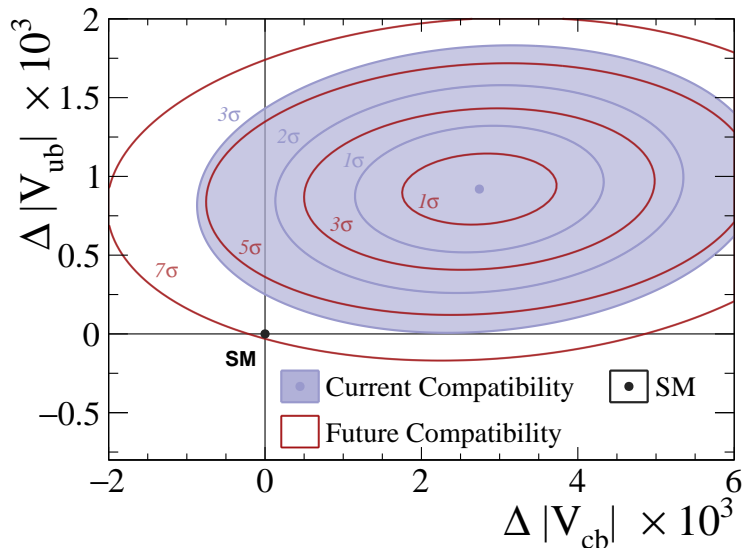

Figure 4: The current (blue) and future (red) compatibilty, at milestone III, of the difference between inclusive and exclusive measurements of $|V_{ub}|$ and $|V_{cb}|$.

of the branching fractions of $B^0 \to D^{(*)+}\tau^-\overline{\nu}_\tau$ to $B^0 \to D^{(*)+}\ell^-\overline{\nu}_\ell$ with $\ell = e$ or μ. Their Standard Model predictions are (0.299 ± 0.03) and (0.257 ± 0.03) respectively [42]. Belle and BaBar have made measurements of both $R(D)$ and $R(D^*)$ [10–14], while LHCb has currently only measured $R(D^*)$ [15, 16]. LHCb also has the potential to measure $R(D)$, but has not yet published such a measurement, hence projections for this are not shown. The
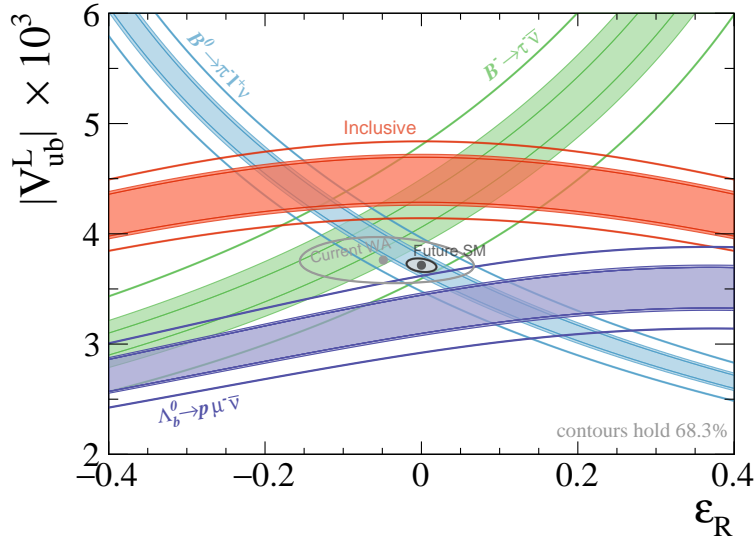
Figure 5: Prospects for new physics measurements related to right-handed currents with the current world averages from Ref. [35] (not filled) and the future projections at milestones I, II and III (filled). The current world average (gray dot and gray line) and the SM point (black dot) with the 1σ exclusion contour at milestone III (black line) are also shown.
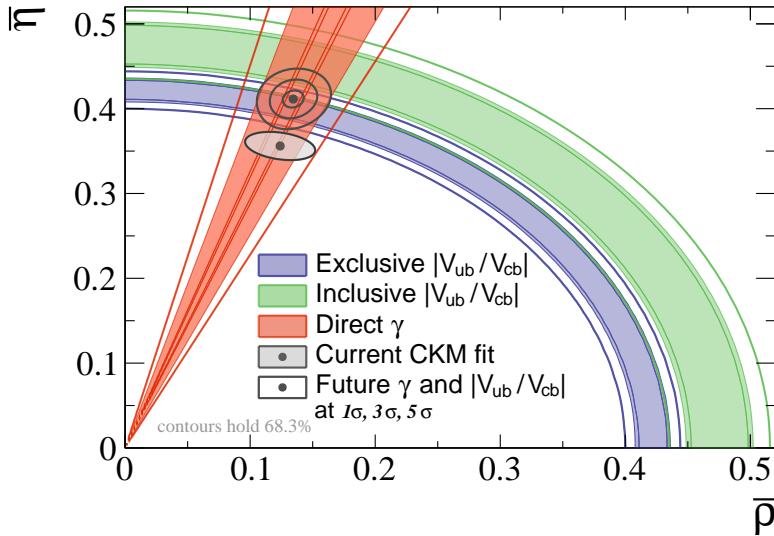
Figure 6: Prospects for CKM fits in $(\overline{\rho}, \overline{\eta})$ space using tree-level processes only with the current world averages from Ref. [35] (not filled) and the future projections of the at milestones I, II and III (filled). The current CKM fit, using all available constraints, from Ref. [38] (gray line with light gray fill) along with the future combination of γ, $|V_{ub}|$ and $|V_{cb}|$ and the 1σ, 3σ and σ exclusion contours at mileston III (dark gray lines with no fill) are also shown.

HFLAV combination of the $R(D^*)$ measurement from LHCb using muonic τ decays with the Belle and BaBar measurements results in a deviation of 3.9σ from the SM prediction [45]. During the writing of this manuscript, LHCb published a second measurement of $R(D^*)$ using hadronic τ decays [16], which was not included as part of the current world average values in this document. The addition of this result is expected to shift the central value of the world average towards the SM predictions slightly, but due to the precision of the measurement, the overall significance of the deviation stays approximately the same. As this effect is expected to be small, we neglect the addition of this measurement and proceed with the current HFLAV world average. The hadronic τ $R(D^*)$ measurement is considered in the future extrapolations.

Complementary measurements have also been made of the ratios $R(K)$ and $R(K^*)$. These ratios differ from $R(D^{(*)})$ as they do not occur at tree level in the SM or involve a τ lepton and therefore probe NP scenarios that couple to different generations of fermions in loop processes. Measurements of $R(K)$ and $R(K^*)$ by the Belle and BaBar experiments are statistically limited [47, 48], however, the LHCb measurements of $R(K)$ and $R(K^*)$ show discrepancies with respect to the SM prediction of around 3σ [18, 19] and are discussed in greater detail in Sec. 4. These measurements, in addition to $R(D)$ and $R(D^*)$, suggest a pattern of tensions among tests of LFU.

The large data samples to be collected by the LHCb and Belle II experiments will be sufficient to confirm the existence of these anomalies, if they are indicative of violation of LFU. In this section, we predict the sensitivity of LHCb and Belle II to $R(D)$ and $R(D^*)$. The central values used for the LHCb and Belle II predictions are taken from the current HFLAV world average [45]. The LHCb $R(D^*)$ statistical uncertainties are scaled from the values measured in the hadronic and muonic channels in Run I according to the expected increase in integrated luminosity, B production cross section and increase in trigger efficiency [27]. Most of the systematic uncertainties are proportional to the data or control samples and are scaled in the same way. However, due to the use of external inputs, there are some irreducible systematics. The external input of the branching fraction of $\tau \to \mu\nu\nu$ to the muonic measurement is not expected to improve in precision from the measurements made at LEP under ideal conditions for τ production using $Z \to \tau\tau$, and hence is kept constant in the future projections at 0.3%. The hadronic measurement relies on external input for the branching fractions of $B^0 \to D^{*+}\pi^-\pi^+\pi^-$ and $B^0 \to D^{*+}\mu^-\overline{\nu}_\mu$, which together contribute 4.8% to the systematic uncertainty. The precision of the branching fraction of $B^0 \to D^*\mu\nu$ is not expected to change since an independent dataset from the one used to measure $R(D)$ and $R(D^*)$ is required. The BaBar measurement of the branching fraction of $B^0 \to D^{*+}\pi^-\pi^+\pi^-$ reconstructs D^{*+} using the $D^{*+} \to D^0\pi^+$ decay with $D^0 \to K^-\pi^+$ [49]. By adding $D^0 \to K^-\pi^+\pi^+\pi^-$, it is expected that the uncertainty can be reduced by 50% in 5 years, reducing the total external systematic to 3.5% in Run III and beyond. The predictions for the Belle II uncertainties are taken from Ref. [28]. The values used are shown in Table 4 and the projection of the future impact is shown in Fig. 7 using the `GammaCombo` package [36]. This shows the significance of the future world average by combining the uncertainties from the SM predictions with the predicted uncertainties of the Belle II and LHCb experiments using their final datasets (with $50\,\mathrm{ab}^{-1}$ at Belle II and $50\,\mathrm{fb}^{-1}$ at LHCb).

Table 4: The SM prediction, world average and predictions of the relative uncertainty of the LHCb and Belle II measurements of $R(D)$ and $R(D^*)$ at $10\,\mathrm{fb}^{-1}$, $22\,\mathrm{fb}^{-1}$ and $50\,\mathrm{fb}^{-1}$ and at $5\,\mathrm{ab}^{-1}$ and $50\,\mathrm{ab}^{-1}$ respectively. LHCb is expected to measure $R(D)$ in the upcoming years.

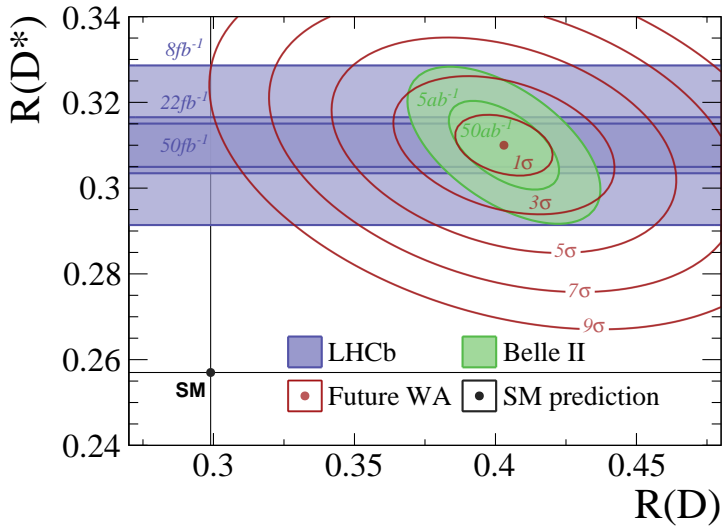| Measurement	SM prediction (Ref. [42])	Current World Average (Ref. [35])	Current Uncertainty (Ref. [35])	Projected Uncertainty				
				Belle II		LHCb		
				$5\,\mathrm{ab}^{-1}$	$50\,\mathrm{ab}^{-1}$	$8\,\mathrm{fb}^{-1}$	$22\,\mathrm{fb}^{-1}$	$50\,\mathrm{fb}^{-1}$
$R(D)$	(0.300 ± 0.003)	$(0.403 \pm 0.040 \pm 0.024)$	11.6%	5.6%	3.2%	-	-	-
$R(D^*)$	(0.252 ± 0.003)	$(0.310 \pm 0.015 \pm 0.008)$	5.5%	3.2%	2.2%	3.6%	2.1%	1.6%

Figure 7: Future prospects for measurements of $R(D)$ and $R(D^*)$. The SM and future expected uncertainties at milestone III are combined to predict the significance with which a given point can be excluded if the current central values remain the same (red lines). The expected uncertainties from Belle II (green) and LHCb (blue) alone are shown as the shaded bands.

It is clear that if the central values remain the same then the statistical power of the Belle II and LHCb experiments will be more than sufficient to reach 5σ. An additional figure in Appendix A, Fig. 10, compares the current world average with the current SM prediction, alongside the projections for Belle II and LHCb.

4   New physics in electroweak penguins

In this section, prospects for new physics searches in $b \to s$ transitions are studied under the SM hypothesis as well as in several NP scenarios, with special attention to present "anomalies". The future projections for Belle II are reported in Ref. [28]. The future uncertainties for LHCb have been symmetrised where appropriate and comprise the decrease

of both statistical and systematic uncertainties as a consequence of the increase in luminosity and the expected improvement in trigger rates [27] for the milestones at $22\,\text{fb}^{-1}$ and $50\,\text{fb}^{-1}$ at centre-of-mass energies of $\sqrt{s} = 14\,\text{TeV}$. For the branching fraction of $B_s^0 \to \phi\gamma$ measured at LHCb [50], the uncertainty on f_s/f_d is assumed to be irreducible.

Estimates of branching fraction ratios, $R(X)$, rely on extrapolations from the muonic branching fractions assuming the same ratio of efficiencies between the electron and muon modes as has been observed in the analysis of $R(K)$ [17].

For current measurements, correlations are taken into account when available. For the theoretical uncertainties on $b \to s\ell^+\ell^-$ exclusive decays, we assume an improvement by a factor of two in hadronic form factors for the extrapolations to the milestones at $50\,\text{ab}^{-1}$ (Belle II) and $22\,\text{fb}^{-1}$ and $50\,\text{fb}^{-1}$ (LHCb), anticipating advancements in lattice QCD.

For $b \to s\ell^+\ell^-$ and radiative $b \to s\gamma$ transitions, the effective Hamiltonian can be expressed as

$$\mathcal{H}_{\text{eff}} = -\frac{4G_F}{\sqrt{2}}\lambda_t \sum_i (C_i O_i + C_i' O_i') + \text{h.c.}, \tag{4.1}$$

where G_F is the Fermi constant and $\lambda_t = V_{tb}V_{ts}^*$ is a CKM factor. In a large class of new physics models, the most important new physics effects in these transitions appear in the Wilson coefficients C_i of the following dimension-6 operators,

$$O_S = \frac{e}{16\pi^2}m_b(\bar{s}P_Rb)(\bar{\ell}\ell), \tag{4.2}$$

$$O_S' = \frac{e^2}{16\pi^2}m_b(P_R\bar{s}b)(\bar{\ell}\gamma_5\ell), \tag{4.3}$$

$$O_P = \frac{e}{16\pi^2}m_b(\bar{s}P_Rb)(\bar{\ell}\ell), \tag{4.4}$$

$$O_P' = \frac{e^2}{16\pi^2}m_b(P_R\bar{s}b)(\bar{\ell}\gamma_5\ell), \tag{4.5}$$

$$O_7 = \frac{e}{16\pi^2}m_b(\bar{s}\sigma^{\mu\nu}P_Rb)F_{\mu\nu}, \tag{4.6}$$

$$O_7' = \frac{e^2}{16\pi^2}m_b(\bar{s}\sigma^{\mu\nu}P_Lb)F_{\mu\nu}, \tag{4.7}$$

$$O_9 = \frac{e}{16\pi^2}(\bar{s}\gamma_\mu P_Lb)(\bar{\ell}\gamma^\mu\ell), \tag{4.8}$$

$$O_9' = \frac{e^2}{16\pi^2}(\bar{s}\gamma_\mu P_Rb)(\bar{\ell}\gamma^\mu\ell), \tag{4.9}$$

$$O_{10} = \frac{e^2}{16\pi^2}(\bar{s}\gamma_\mu P_Lb)(\bar{\ell}\gamma^\mu\gamma_5\ell), \tag{4.10}$$

$$O_{10}' = \frac{e^2}{16\pi^2}(\bar{s}\gamma_\mu P_Rb)(\bar{\ell}\gamma^\mu\gamma_5\ell). \tag{4.11}$$

In the following considerations, the effective Wilson coefficient C_7^{eff} (see e.g. [51]) is used instead of C_7 as this effective coefficient is independent of the regularisation scheme, where we define

Table 5: New physics scenarios for LHCb, Belle II exclusive and Belle II inclusive Wilson coefficient scans. Contributions to the Wilson coefficients arising from new physics are given for each scan.

	$(C_9^{\mathrm{NP}\mu\mu}, C_{10}^{\mathrm{NP}\mu\mu})$	$(C_9'^{\mu\mu}, C_{10}'^{\mu\mu})$	$(C_9^{\mathrm{NP}\mu\mu}, C_9^{\mathrm{NP}ee})$	$(\mathcal{R}e\left(C_7'^{\mathrm{NP}}\right), \mathcal{I}m\left(C_7'^{\mathrm{NP}}\right))$	$(\mathcal{R}e\left(C_7^{\mathrm{NP}}\right), \mathcal{I}m\left(C_7^{\mathrm{NP}}\right))$
LHCb	$(-1.0, 0.0)$	$(-0.2, -0.2)$	$(-1.0, 0.0)$	$(0.00, 0.04)$	$(-0.075, 0.000)$
Belle II exclusive	$(-1.4, 0.4)$	$(0.4, 0.2)$	$(-1.4, -0.7)$	$(0.08, 0.00)$	$(-0.050, 0.050)$
Belle II inclusive	$(-0.8, 0.6)$	$(0.8, 0.2)$	$(-0.8, 0.4)$	$(0.02, -0.06)$	$(-0.050, -0.075)$

$$C_7^{\mathrm{eff}} = C_7^{\mathrm{eff\,SM}} + C_7^{\mathrm{NP}}, \tag{4.12}$$

$$C_7'^{\mathrm{eff}} = C_7'^{\mathrm{eff\,SM}} + C_7'^{\mathrm{NP}}. \tag{4.13}$$

The impact of future measurements is studied by performing scans of the new physics contribution of Wilson coefficients at a scale of $\mu = 4.8\,\mathrm{GeV}$ under different new physics scenarios and the SM hypothesis using `flavio` [52]. To allow for a proper comparison and because the uncertainties have different origins, the measurements are divided into inclusive and exclusive measurements, wherefore different NP scenarios are chosen for each class of measurement and each scan, on the basis of existing global fits [53–58]. Scans to C_S and C_P are omitted as these are dominated by contributions from purely leptonic $B \to \ell^+\ell^-$ decays, where, apart from for $B_s^0 \to \mu^+\mu^-$, only limits are available.

The scans of the electromagnetic dipole coefficients $C_7^{(\prime)}$ rely on measurements of the branching fractions of $B_s^0 \to \phi\gamma$, $B^+ \to K^{*+}\gamma$, $B^0 \to K^{*0}\gamma$, $B \to X_s\gamma$, on $\mathcal{A}^{\Delta\Gamma}(B_s^0 \to \phi\gamma)$ and $S_{K^*\gamma}$ as well as $A_T^{(2)}$ (also known as P_1) and A_T^{Im} extracted from $B^0 \to K^{*0}e^+e^-$ decays at very low q^2. Furthermore, the angular observables $A_{7,8,9}$ in $B^0 \to K^{*0}\mu^+\mu^-$ constrain the imaginary part of $C_7^{(\prime)}$.

The measurements entering the scans of the semi-leptonic coefficients $C_{9,10}^{(\prime)}$ comprise the inclusive $\mathcal{B}(B \to X_s\mu^+\mu^-)$ at low and high q^2; the low q^2 range is split equally for extrapolations. The forward-backward asymmetry $A_{\mathrm{FB}}(B \to X_s\ell^+\ell^-)$ has been measured at low and high q^2, and extrapolations to future sensitivities are available in several low and high q^2 ranges. The differential branching fractions $d\mathcal{B}/dq^2$ of $B^+ \to K^+\mu^+\mu^-$, $B^0 \to K^{*0}\mu^+\mu^-$ and $B_s^0 \to \phi\mu^+\mu^-$ decays in both low and high q^2 regions is included in the scans, as well as the angular observables $S_{3,4,5}, F_L, A_{\mathrm{FB}}$ in several bins of q^2 from LHCb. The angular observables available for Belle (II) are $P_{4,5}'(B^0 \to K^{*0}\mu^+\mu^-)$ in similar ranges. Scans of $C_{10}^{(\prime)}$ further include the branching fraction of the decay $B_s^0 \to \mu^+\mu^-$.

In the scan of $C_9^{\mathrm{NP}\mu\mu}$ vs. $C_9^{\mathrm{NP}ee}$, $P_{4,5}'$ extracted from $B^0 \to K^{*0}e^+e^-$ decays is included in addition to the muonic final state. Information on electrons is further obtained from the ratios of branching fraction between muon and electron final states for $R(X_s), R(K), R(K^*)$ and $R(\phi)$. The results of the Belle collaboration on $R(K)$ and $R(K^*)$ in the region $0.0 < q^2 < 22.0\,\mathrm{GeV}^2$ were not considered as input in this scan as the charmonium region is included [47]. The inclusive measurement of $R(X_s)$ will become accessible at Belle II,

whereas $R(\phi)$ will be measurable at LHCb at low and high q^2. Measurements of lepton flavour universality pose stringent tests on the SM as several tensions have been observed. The LHCb collaboration found $R(K)$ to be $0.745^{+0.090}_{-0.074} \pm 0.036$ [17]; 2.6σ below the SM expectation. The symmetrised uncertainty on $R(K)$ in $1.0 < q^2 < 6.0\,\text{GeV}^2$ is expected to be 0.046 after $8\,\text{fb}^{-1}$, 0.025 after $22\,\text{fb}^{-1}$ and down to 0.016 after LHCb has recorded $50\,\text{fb}^{-1}$ of data. The uncertainties in $15.0 < q^2 < 22.0\,\text{GeV}^2$ are expected to behave similarly. A recent measurement of $R(K^*)$ by the LHCb collaboration [18] finds a tension of $2.1 - 2.3\sigma$ in $0.045 < q^2 < 1.1\,\text{GeV}^2$ and of $2.4 - 2.5\sigma$ in $1.1 < q^2 < 6.0\,\text{GeV}^2$ with respect to the available SM predictions. The measured values of $R(K^*)$ are $0.66^{+0.11}_{-0.07} \pm 0.03$ in the very low and $0.69^{+0.11}_{-0.07} \pm 0.05$ in the low q^2 regions [18]. The symmetrised uncertainties are extrapolated to future datasets and expected to be $0.048\,(0.053)$, $0.026\,(0.028)$ and $0.017\,(0.019)$ after $8\,\text{fb}^{-1}, 22\,\text{fb}^{-1}$, and $50\,\text{fb}^{-1}$, respectively, for low (central) q^2 regions. If the anomalies in $R(K)$ and $R(K^*)$ persist at the current central values, LHCb will measure $R(K)$ with a significance of $> 5\sigma$ with respect to the SM prediction after $8\,\text{fb}^{-1}$, increasing to 15σ with the $50\,\text{fb}^{-1}$ dataset. Concerning $R(K^*)$ at low q^2, the tension would increase to $3.4 - 3.8\sigma\,(6.2 - 6.9\sigma)$ depending on the SM prediction after Run 2 (Run 3); a tension of around 10σ would be reached after Run 4. For $R(K^*)$ at high q^2, a tension of $4.7 - 4.8\sigma$ would emerge after $8\,\text{fb}^{-1}$ increasing to $9.0 - 9.1\sigma\,(13.2 - 13.4\sigma)$ after $22\,(50)\,\text{fb}^{-1}$. If the anomalies in $b \to s\ell^+\ell^-$ decays persist, the Belle II collaboration will be able to confirm the anomalies in $R(K)\,(R(K^*))$ with $50\,\text{ab}^{-1}$ in the region $1.0\,(1.1) < q^2 < 6.0\,\text{GeV}^2$ with significances around $7 - 8\sigma$ and hence, a conclusive tension will be observed within the next years.

The scans of the unprimed semi-leptonic and electromagnetic dipole Wilson coefficients are illustrated in Fig. 8, where detailed information on the chosen inputs together with the scans of the primed operators are given in Appendix B. As illustrated in Figs. 13(a) and 13(b), no discrepancies to the SM for the primed operators is visible. The electromagnetic dipole operators seem to behave as expected from the SM and the contours obtained from LHCb, inclusive and exclusive Belle II measurements are in good agreement.

The current measurements hint at a deviation of the unprimed operator $C_9^{\text{NP}\mu\mu}$ from the SM values as $C_9^{\text{NP}\mu\mu}$ prefers a negative value, which is driven by the LHCb measurements. In contrast to the tension observed in $C_9^{\text{NP}\mu\mu}$, no hints towards new physics are visible in $C_9^{\text{NP}ee}$ nor in $C_{10}^{\text{NP}\mu\mu}$. If the current anomaly in $C_9^{\text{NP}\mu\mu}$ persists, the combined sensitivity of LHCb with $50\,\text{fb}^{-1}$ and Belle II with $50\,\text{ab}^{-1}$ will allow for clarification of whether there is a new physics contribution to $C_9^{\text{NP}\mu\mu}$.

Even if the curent tensions seen in $b \to s\ell^+\ell^-$ data turn out to be statistical fluctuations, there are many very rare decays, lepton flavour violating decays, and decays with neutrinos in the final state that are orthogonal clean probes of NP. Corresponding sensitivities are listed in Table 6. For the determination of the sensitivity of $B_s^0 \to \tau^+\tau^-$, the conservative assumption of the same trigger improvement as for a decay with a single tau lepton was used. The extrapolations of $B_s^0 \to e^+e^-$ are extracted from the latest LHCb measurement [59] of $B_s^0 \to \mu^+\mu^-$ by factoring in an electron penalty factor. Following the approach in [60], the τ production cross section was scaled linearly with the centre-of-mass energy.
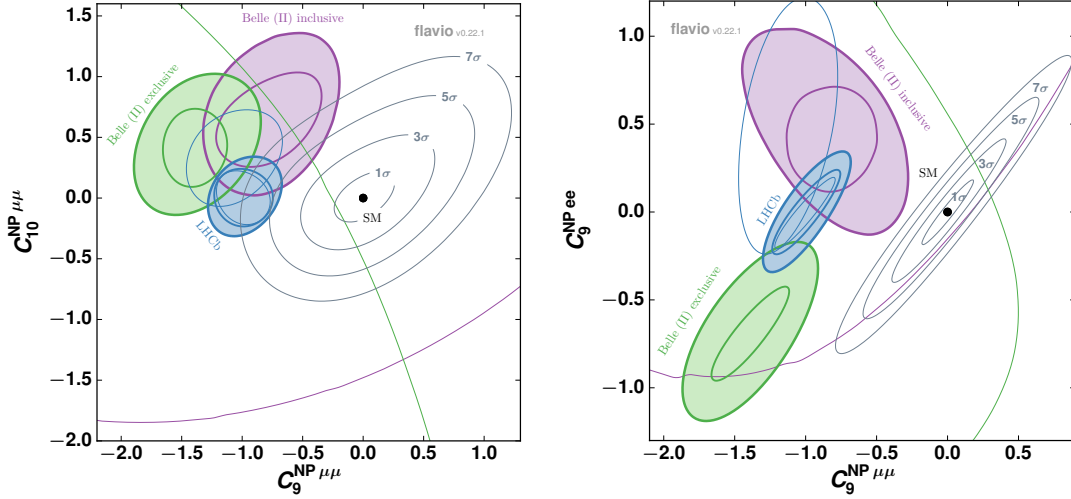
(a) $C_9^{\mathrm{NP}\mu\mu}$ versus $C_{10}^{\mathrm{NP}\mu\mu}$.

(b) $C_9^{\mathrm{NP}\mu\mu}$ versus $C_9^{\mathrm{NP}ee}$.
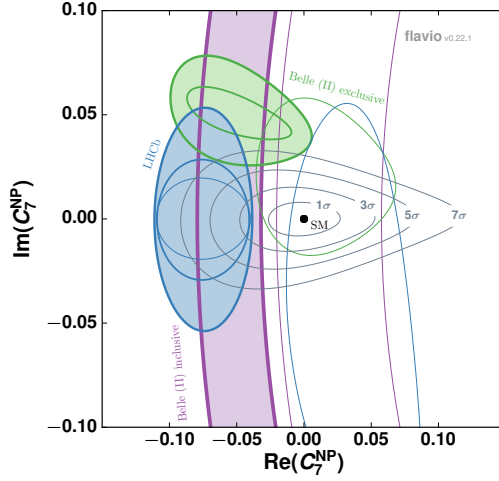
(c) $\mathcal{R}e\left(C_7^{\mathrm{NP}}\right)$ versus $\mathcal{I}m\left(C_7^{\mathrm{NP}}\right)$.

Figure 8: In the two-dimensional scans of pairs of Wilson coefficients, the current average (not filled) as well as the extrapolations to future sensitivities (filled) of LHCb after $8, 22, 50\,\mathrm{fb}^{-1}$ (exclusive) and Belle II after $5, 50\,\mathrm{ab}^{-1}$ (inclusive and exclusive) are given. The central values of the extrapolations have been evaluated in the NP scenarios listed in Table 5. The contours correspond to 1σ uncertainty bands. The Standard Model point (black dot) with the $1\sigma, 3\sigma, 5\sigma$ and 7σ exclusion contours with a combined sensitivity of LHCb's $50\,\mathrm{fb}^{-1}$ and Belle II's $50\,\mathrm{ab}^{-1}$ datasets is indicated in light grey. The primed operators show no tensions with respect to the SM; hence no SM exclusions are provided.

Table 6: Expected sensitivities of specific very rare decays; limits are given at 90% C. L. . Note that Belle II has sensitivity for $B_s^0 \to \ell^+\ell^-$, but we only consider the impact of the $e^+e^- \to \Upsilon(4S) \to B\bar{B}$ data taking in this study. The extrapolations of $B_s^0 \to \mu^+\mu^-$ refer to the combined statistical and systematic uncertainty and are based on the latest LHCb measurement on a dataset corresponding to an integrated luminosity of $4.4\,\mathrm{fb}^{-1}$ [59].

	current	LHCb $8\,\mathrm{fb}^{-1}$	$22\,\mathrm{fb}^{-1}$	$50\,\mathrm{fb}^{-1}$	Belle II $50\,\mathrm{ab}^{-1}$
$B_s^0 \to \mu^+\mu^-$	$(2.4^{+0.9}_{-0.7}) \times 10^{-9}$ [35][iii]	0.45×10^{-9}	0.24×10^{-9}	0.16×10^{-9}	-
$B^0 \to \mu^+\mu^-$	$< 0.28 \times 10^{-9}$ [59][iv]	$< 0.19 \times 10^{-9}$	$< 0.10 \times 10^{-9}$	$< 0.07 \times 10^{-9}$	$< 5 \times 10^{-9}$
$B_s^0 \to e^+e^-$	$< 2.8 \times 10^{-7}$ [61]	$< 0.27 \times 10^{-8}$	$< 0.12 \times 10^{-8}$	$< 0.07 \times 10^{-8}$	-
$B^0 \to e^+e^-$	$< 8.3 \times 10^{-8}$ [61]	$< 0.12 \times 10^{-8}$	$< 0.05 \times 10^{-8}$	$< 0.03 \times 10^{-8}$	$< 3 \times 10^{-9}$
$B_s^0 \to \tau^+\tau^-$	$< 5.2 \times 10^{-3}$ [62]	$< 2.7 \times 10^{-3}$	$< 0.9 \times 10^{-3}$	$< 0.5 \times 10^{-3}$	-
$B^0 \to \tau^+\tau^-$	$< 1.6 \times 10^{-3}$ [62]	$< 0.8 \times 10^{-3}$	$< 0.3 \times 10^{-3}$	$< 0.2 \times 10^{-3}$	$< 0.3 \times 10^{-3}$
$B_s^0 \to e^\pm\mu^\mp$	$< 1.1 \times 10^{-8}$ [63][v]	$< 0.31 \times 10^{-8}$	$< 0.15 \times 10^{-8}$	$< 0.10 \times 10^{-8}$	-
$B^0 \to e^\pm\mu^\mp$	$< 2.8 \times 10^{-9}$ [63][v]	$< 0.8 \times 10^{-9}$	$< 0.4 \times 10^{-9}$	$< 0.2 \times 10^{-9}$	$< 4.0 \times 10^{-9}$
$\tau^- \to \mu^+\mu^-\mu^-$	$< 2.1 \times 10^{-8}$ [64]	$< 2.4 \times 10^{-8}$ [60]	$< 1.3 \times 10^{-8}$	$< 0.8 \times 10^{-8}$	$< 3.5 \times 10^{-10}$
$\tau^- \to \mu^-\gamma$	$< 4.4 \times 10^{-8}$ [65]	-	-	-	$< 1.0 \times 10^{-9}$
$B^+ \to K^+\nu\bar{\nu}$	$< 1.6 \times 10^{-5}$ [66]	-	-	-	10.7% [67]
$B^+ \to K^{*+}\nu\bar{\nu}$	$< 4.0 \times 10^{-5}$ [68]	-	-	-	9.3% [67]
$B^0 \to K^{*0}\nu\bar{\nu}$	$< 5.5 \times 10^{-5}$ [68]	-	-	-	9.6% [67]

[iii] This average does not contain the latest LHCb measurement [59].
[iv] From supplementary material. A combination of measurements is available from [35].
[v] This measurement has been performed on 1 fb^{-1} and has been extrapolated to $3\,\mathrm{fb}^{-1}$.

5   Conclusion

We analysed projections of the sensitivity of the future Belle II and LHCb datasets to be collected in the upcoming years, until the end of Belle II data taking and the end of the planned LHCb phase 1 upgrade. The foreseen changes in the trigger system of LHCb are considered as well as the anticipated scaling of the systematic uncertainties. This manuscript focuses on present day anomalies and key measurements in the flavour sector such as the parameters of the CKM matrix, which need to be determined experimentally. Amongst the most interesting parameters to measure are the side of the CKM matrix which is proportional to $|V_{ub}|/|V_{cb}|$ and the CKM angle γ, where the latter will be measured to a precision of below $1°$. There has been a long standing discrepancy between the inclusive and exclusive determination of $|V_{ub}|$ (and to some extent also $|V_{cb}|$), which will, if the current central values remain, be established with a significance well beyond 5σ. Further tensions have been observed in tests of lepton flavour universality in tree-level and loop-level processes. The current HFLAV average of the ratio of $B \to D^{(*)}\ell\nu$ tree-level decays involving τ leptons and light leptons, $R(D)$ and $R(D^*)$, differs from the Standard Model prediction by 3.9σ. The future measurements will yield precisions of 3.2% and 1.3%, for $R(D)$ and $R(D^*)$ respectively (which does not include the potential for LHCb to also

measure $R(D)$). If the current central values persist, the SM prediction can be ruled out by the combined dataset of Belle II and LHCb with a significance of well beyond 10σ. Further hints at a possible violation of lepton flavour universality have emerged in flavour-changing neutral current decays based on $b \to s$ transitions, which are a sensitive probe of new physics. The reach of the future experiments is analysed by a scan of the Wilson coefficients under different new physics scenarios and the SM hypothesis. Currently, a set of anomalies in a range of observables from lepton flavour universality to branching ratio and angular observables is seen with local significances ranging between $2.5 - 3.9\sigma$. The current combination of these anomalies is reported by several groups performing global fits, some of which quote deviations with a significance well beyond five standard deviations. However, depending on the treatment of hadronic uncertainties, the significance can be considerably less. More data and more work on the theoretical side are needed to clarify the situation. If the anomalies in $b \to s\ell^+\ell^-$ decays persist, a highly significant tension will be observed within the next years by the two single experiments independently.

Even though both the Belle II and the LHCb experiments could individually confirm or rule out the current flavour anomalies, the great advantage of the current experimental situation is that a potential anomaly can immediately be checked by a competing experiment with mostly orthogonal systematic uncertainties. Both experiments furthermore have different strengths, for example in inclusive measurements or measurements involving neutral final states for Belle II and for exclusive measurements or measurements involving very rare decays at LHCb.

We conclude that flavour observables currently showing anomalies will be precisely measured by the Belle II and LHCb collaborations in the upcoming years allowing conclusions to be drawn on their nature. If the central values remain at the current values, discoveries with significances well above five standard deviations will be made for several important flavour physics anomalies.

6   Acknowledgements

References

[1] **BaBar** Collaboration, B. Aubert et al., *The BABAR detector*, *Nucl. Instrum. and Meth.* **A479** (01, 2002) 1–116.

[2] **Belle** Collaboration, A. Abashian et al., *The Belle Detector*, *Nucl. Instrum. Meth.* **A479** (2002) 117–232.

[3] **LHCb** Collaboration, A. A. Alves, Jr. et al., *The LHCb Detector at the LHC*, *JINST* **3** (2008) S08005.

[4] G. Ciezarek, M. Franco Sevilla, B. Hamilton, R. Kowalewski, T. Kuhr, V. Lüth, and Y. Sato, *A Challenge to Lepton Universality in B Meson Decays*, *Nature* **546** (2017) 227–233, [arXiv:1703.01766].

[5] F. Archilli, M.-O. Bettler, P. Owen, and K. A. Petridis, *Flavour-changing neutral currents making and breaking the standard model*, *Nature* **546** (2017) 221–226.

[6] **Belle-II** Collaboration, T. Abe et al., *Belle II Technical Design Report*, arXiv:1011.0352.

[7] **LHCb** Collaboration, I. Bediaga et al., *Framework TDR for the LHCb Upgrade: Technical Design Report*, Tech. Rep. CERN-LHCC-2012-007, 2012.

[8] N. Cabibbo, *Unitary symmetry and leptonic decays*, *Phys.Rev.Lett.* **10** (1963) 531–533.

[9] M. Kobayashi and T. Maskawa, *CP violation in the renormalizable theory of weak interaction*, *Prog.Theor.Phys.* **49** (1973) 652–657.

[10] **BaBar** Collaboration, J. P. Lees et al., *Evidence for an excess of $\bar{B} \to D^{(*)}\tau^-\bar{\nu}_\tau$ decays*, *Phys. Rev. Lett.* **109** (2012) 101802, [arXiv:1205.5442].

[11] **BaBar** Collaboration, J. P. Lees et al., *Measurement of an Excess of $\bar{B} \to D^{(*)}\tau^-\bar{\nu}_\tau$ Decays and Implications for Charged Higgs Bosons*, *Phys. Rev.* **D88** (2013), no. 7 072012, [arXiv:1303.0571].

[12] **Belle** Collaboration, M. Huschle et al., *Measurement of the branching ratio of $\bar{B} \to D^{(*)}\tau^-\bar{\nu}_\tau$ relative to $\bar{B} \to D^{(*)}\ell^-\bar{\nu}_\ell$ decays with hadronic tagging at Belle*, *Phys. Rev.* **D92** (2015), no. 7 072014, [arXiv:1507.03233].

[13] **Belle** Collaboration, Y. Sato et al., *Measurement of the branching ratio of $\bar{B}^0 \to D^{*+}\tau^-\bar{\nu}_\tau$ relative to $\bar{B}^0 \to D^{*+}\ell^-\bar{\nu}_\ell$ decays with a semileptonic tagging method*, *Phys. Rev.* **D94** (2016), no. 7 072007, [arXiv:1607.07923].

[14] **Belle** Collaboration, S. Hirose et al., *Measurement of the τ lepton polarization and $R(D^*)$ in the decay $\bar{B} \to D^*\tau^-\bar{\nu}_\tau$*, arXiv:1612.00529.

[15] **LHCb** Collaboration, R. Aaij et al., *Measurement of the ratio of branching fractions $\mathcal{B}(\bar{B}^0 \to D^{*+}\tau^-\bar{\nu}_\tau)/\mathcal{B}(\bar{B}^0 \to D^{*+}\mu^-\bar{\nu}_\mu)$*, *Phys. Rev. Lett.* **115** (2015), no. 11 111803, [arXiv:1506.08614]. [Addendum: Phys. Rev. Lett.115,no.15,159901(2015)].

[16] **LHCb** Collaboration, R. Aaij et al., *Measurement of the ratio of the $B^0 \to D^{*-}\tau^+\nu_\tau$ and $B^0 \to D^{*-}\mu^+\nu_\mu$ branching fractions using three-prong τ-lepton decays*, arXiv:1708.08856.

[17] **LHCb** Collaboration, R. Aaij et al., *Test of lepton universality using $B^+ \to K^+\ell^+\ell^-$ decays*, *Phys. Rev. Lett.* **113** (2014) 151601, [arXiv:1406.6482].

[18] **LHCb** Collaboration, R. Aaij et al., *Test of lepton universality with $B^0 \to K^{*0}\ell^+\ell^-$ decays*, *JHEP* **08** (2017) 055, [arXiv:1705.05802].

[19] **LHCb** Collaboration, R. Aaij et al., *Differential branching fractions and isospin asymmetries of $B \to K^{(*)}\mu^+\mu^-$ decays*, *JHEP* **06** (2014) 133, [arXiv:1403.8044].

[20] **LHCb** Collaboration, R. Aaij et al., *Measurement of the phase difference between short- and long-distance amplitudes in the $B^+ \to K^+\mu^+\mu^-$ decay*, *Eur. Phys. J.* **C77** (2017), no. 3 161, [arXiv:1612.06764].

[21] **LHCb** Collaboration, R. Aaij et al., *Angular analysis of the $B^0 \to K^{*0}\mu^+\mu^-$ decay using 3 fb^{-1} of integrated luminosity*, *JHEP* **02** (2016) 104, [arXiv:1512.04442].

[22] **Belle** Collaboration, S. Wehle et al., *Lepton-Flavor-Dependent Angular Analysis of $B \to K^*\ell^+\ell^-$*, *Phys. Rev. Lett.* **118** (2017), no. 11 111801, [arXiv:1612.05014].

[23] **LHCb** Collaboration, R. Aaij et al., *Angular analysis and differential branching fraction of the decay $B_s^0 \to \phi\mu^+\mu^-$*, *JHEP* **09** (2015) 179, [arXiv:1506.08777].

[24] **LHCb** Collaboration, R. Aaij et al., *Differential branching fraction and angular analysis of $\Lambda_b^0 \to \Lambda\mu^+\mu^-$ decays*, *JHEP* **06** (2015) 115, [arXiv:1503.07138].

[25] **LHCb** Collaboration, R. Aaij et al., *Measurement of B meson production cross-sections in proton-proton collisions at $\sqrt{s} = 7$ TeV*, *JHEP* **08** (2013) 117, [arXiv:1306.3663].

[26] **LHCb** Collaboration, R. Aaij et al., *Measurement of the b-quark production cross-section in 7 and 13 TeV pp collisions*, *Phys. Rev. Lett.* **118** (2017), no. 5 052002, [arXiv:1612.05140].

[27] **LHCb** Collaboration, *LHCb Trigger and Online Upgrade Technical Design Report*, Tech. Rep. CERN-LHCC-2014-016, 2014.

[28] E. Kou, P. Urquijo, Belle II collaboration and the B2Tip theory community, *The Belle II Physics Book*, *To appear* (2017).

[29] *Medium-Term Plan for the period 2016-2020. 294th Meeting of Scientific Policy Committee*, Tech. Rep. CERN/SPC/1050, CERN/FC/5932, CERN/3197, 2015.

[30] **LHCb** Collaboration, *Expression of Interest for a Phase-II LHCb Upgrade: Opportunities in flavour physics, and beyond, in the HL-LHC era*, Tech. Rep. CERN-LHCC-2017-003, Geneva, 2017.

[31] J. Brod, A. Lenz, G. Tetlalmatzi-Xolocotzi, and M. Wiebusch, *New physics effects in tree-level decays and the precision in the determination of the quark mixing angle γ*, *Phys. Rev.* **D92** (2015), no. 3 033002, [arXiv:1412.1446].

[32] **Belle** Collaboration, A. Sibidanov et al., *Study of Exclusive $B \to X_u\ell\nu$ Decays and Extraction of $|V_{ub}|$ using Full Reconstruction Tagging at the Belle Experiment*, *Phys. Rev.* **D88** (2013), no. 3 032005, [arXiv:1306.2781].

[33] **Belle** Collaboration, R. Glattauer et al., *Measurement of the decay $B \to D\ell\nu_\ell$ in fully reconstructed events and determination of the Cabibbo-Kobayashi-Maskawa matrix element $|V_{cb}|$*, *Phys. Rev.* **D93** (2016), no. 3 032006, [arXiv:1510.03657].

[34] **LHCb** Collaboration, R. Aaij et al., *Determination of the quark coupling strength $|V_{ub}|$ using baryonic decays*, *Nature Phys.* **11** (2015) 743–747, [arXiv:1504.01568].

[35] **Particle Data Group** Collaboration, C. Patrignani et al., *Review of particle physics*, *Chin. Phys.* **C40** (2016) 100001.

[36] M. Kenzie, "GammaCombo - A statistical analysis framework for combining measurements, fitting datasets and producing confidence intervals." https://gammacombo.github.io.

[37] A. Crivellin, *Effects of right-handed charged currents on the determinations of* $|V_{ub}|$ *and* $|V_{cb}|$, *Phys. Rev.* **D81** (2010) 031301, [arXiv:0907.2461].

[38] **CKMfitter group** Collaboration, J. Charles et al., *CP violation and the CKM matrix: Assessing the impact of the asymmetric B factories*, *Eur.Phys.J.* **C41** (2005) 1–131, [hep-ph/0406184]. updated results and plots available at: http://ckmfitter.in2p3.fr.

[39] D. Bigi, P. Gambino, and S. Schacht, *A fresh look at the determination of* $|V_{cb}|$ *from* $B \to D^* \ell \nu$, *Phys. Lett.* **B769** (2017) 441–445, [arXiv:1703.06124].

[40] B. Grinstein and A. Kobach, *Model-Independent Extraction of* $|V_{cb}|$ *from* $\bar{B} \to D^* \ell \overline{\nu}$, *Phys. Lett.* **B771** (2017) 359–364, [arXiv:1703.08170].

[41] I. Caprini, L. Lellouch, and M. Neubert, *Dispersive bounds on the shape of* $\overline{B} \to D^{(*)} \ell \overline{\nu}_\ell$ *form-factors*, *Nucl. Phys.* **B530** (1998) 153–181, [hep-ph/9712417].

[42] F. U. Bernlochner, Z. Ligeti, M. Papucci, and D. J. Robinson, *Combined analysis of semileptonic B decays to D and* D^*: $R(D^{(*)})$, $|V_{cb}|$, *and new physics*, *Phys. Rev.* **D95** (2017), no. 11 115008, [arXiv:1703.05330].

[43] C. G. Boyd, B. Grinstein, and R. F. Lebed, *Precision corrections to dispersive bounds on form-factors*, *Phys. Rev.* **D56** (1997) 6895–6911, [hep-ph/9705252].

[44] F. U. Bernlochner, Z. Ligeti, M. Papucci, and D. J. Robinson, *Tensions and correlations in* $|V_{cb}|$ *determinations*, arXiv:1708.07134.

[45] Y. Amhis et al., *Averages of b-hadron, c-hadron, and* τ*-lepton properties as of summer 2016*, arXiv:1612.07233.

[46] **LHCb** Collaboration, R. Aaij et al., *Measurement of the CKM angle* γ *from a combination of LHCb results*, *JHEP* **12** (2016) 087, [arXiv:1611.03076].

[47] **Belle** Collaboration, J. T. Wei et al., *Measurement of the Differential Branching Fraction and Forward-Backword Asymmetry for* $B \to K^{(*)} \ell^+ \ell^-$, *Phys. Rev. Lett.* **103** (2009) 171801, [arXiv:0904.0770].

[48] **BaBar** Collaboration, B. Aubert et al., *Direct CP, Lepton Flavor and Isospin Asymmetries in the Decays* $B \to K^{(*)} \ell^+ \ell^-$, *Phys. Rev. Lett.* **102** (2009) 091803, [arXiv:0807.4119].

[49] **BaBar** Collaboration, J. P. Lees et al., *Measurement of the* $B^0 \to D^{*-} \pi^+ \pi^- \pi^+$ *branching fraction*, *Phys. Rev.* **D94** (2016), no. 9 091101, [arXiv:1609.06802].

[50] **LHCb** Collaboration, R. Aaij et al., *Measurement of the ratio of branching fractions* $BR(B_0 \to K^{\star 0} \gamma)/BR(B_{s0} \to \phi \gamma)$ *and the direct CP asymmetry in* $B_0 \to K^{\star 0} \gamma$, *Nucl. Phys.* **B867** (2013) 1–18, [arXiv:1209.0313].

[51] T. Blake, G. Lanfranchi, and D. M. Straub, *Rare B Decays as Tests of the Standard Model*, *Prog. Part. Nucl. Phys.* **92** (2017) 50–91, [arXiv:1606.00916].

[52] D. Straub, "flavio - A Python package for flavour physics phenomenology in the Standard Model and beyond." https://flav-io.github.io.

[53] T. Hurth, F. Mahmoudi, and S. Neshatpour, *On the anomalies in the latest LHCb data*, *Nucl. Phys.* **B909** (2016) 737–777, [arXiv:1603.00865].

[54] A. Paul and D. M. Straub, *Constraints on new physics from radiative B decays*, *JHEP* **04** (2017) 027, [arXiv:1608.02556].

[55] B. Capdevila, A. Crivellin, S. Descotes-Genon, J. Matias, and J. Virto, *Patterns of New Physics in* $b \to s \ell^+ \ell^-$ *transitions in the light of recent data*, arXiv:1704.05340.

[56] W. Altmannshofer, C. Niehoff, P. Stangl, and D. M. Straub, *Status of the $B \to K^* \mu^+ \mu^-$ anomaly after Moriond 2017*, Eur. Phys. J. **C77** (2017), no. 6 377, [arXiv:1703.09189].

[57] W. Altmannshofer, P. Stangl, and D. M. Straub, *Interpreting Hints for Lepton Flavor Universality Violation*, Phys. Rev. **D96** (2017), no. 5 055008, [arXiv:1704.05435].

[58] L.-S. Geng, B. Grinstein, S. Jäger, J. Martin Camalich, X.-L. Ren, and R.-X. Shi, *Towards the discovery of new physics with lepton-universality ratios of $b \to s\ell\ell$ decays*, arXiv:1704.05446.

[59] **LHCb** Collaboration, R. Aaij et al., *Measurement of the $B_s^0 \to \mu^+ \mu^-$ branching fraction and effective lifetime and search for $B^0 \to \mu^+ \mu^-$ decays*, Phys. Rev. Lett. **118** (2017), no. 19 191801, [arXiv:1703.05747].

[60] **LHCb** Collaboration, R. Aaij et al., *Searches for violation of lepton flavour and baryon number in tau lepton decays at LHCb*, Phys. Lett. **B724** (2013) 36–45, [arXiv:1304.4518].

[61] **CDF** Collaboration, T. Aaltonen et al., *Search for the Decays $B_s^0 \to e^+ \mu^-$ and $B_s^0 \to e^+ e^-$ in CDF Run II*, Phys. Rev. Lett. **102** (2009) 201801, [arXiv:0901.3803].

[62] **LHCb** Collaboration, R. Aaij et al., *Search for the decays $B_s^0 \to \tau^+ \tau^-$ and $B^0 \to \tau^+ \tau^-$*, Phys. Rev. Lett. **118** (2017), no. 25 251802, [arXiv:1703.02508].

[63] **LHCb** Collaboration, R. Aaij et al., *Search for the lepton-flavor violating decays $B_s^0 \to e^\pm \mu^\mp$ and $B^0 \to e^\pm \mu^\mp$*, Phys. Rev. Lett. **111** (2013) 141801, [arXiv:1307.4889].

[64] K. Hayasaka et al., *Search for Lepton Flavor Violating Tau Decays into Three Leptons with 719 Million Produced Tau+Tau- Pairs*, Phys. Lett. **B687** (2010) 139–143, [arXiv:1001.3221].

[65] **BaBar** Collaboration, B. Aubert et al., *Searches for Lepton Flavor Violation in the Decays $\tau^\pm \to e^\pm \gamma$ and $\tau^\pm \to \mu^\pm \gamma$*, Phys. Rev. Lett. **104** (2010) 021802, [arXiv:0908.2381].

[66] **BaBar** Collaboration, J. P. Lees et al., *Search for $B \to K^{(*)} \nu \bar{\nu}$ and invisible quarkonium decays*, Phys. Rev. **D87** (2013), no. 11 112005, [arXiv:1303.7465].

[67] E. Manoni, "Studies of missing energy decays of B meson at Belle II." https://indico.cern.ch/event/466934/contributions/2582030/, July, 2017.

[68] **Belle** Collaboration, O. Lutz et al., *Search for $B \to h^{(*)} \nu \bar{\nu}$ with the full Belle $\Upsilon(4S)$ data sample*, Phys. Rev. **D87** (2013), no. 11 111103, [arXiv:1303.3719].

[69] **Belle** Collaboration, A. Abdesselam et al., *Measurement of the inclusive $B \to X_{s+d} \gamma$ branching fraction, photon energy spectrum and HQE parameters*, in *Proceedings, 38th International Conference on High Energy Physics (ICHEP 2016): Chicago, IL, USA, August 3-10, 2016*, 2016. arXiv:1608.02344.

[70] **BaBar** Collaboration, J. P. Lees et al., *Measurement of the $B \to X_s l^+ l^-$ branching fraction and search for direct CP violation from a sum of exclusive final states*, Phys. Rev. Lett. **112** (2014) 211802, [arXiv:1312.5364].

[71] **Belle** Collaboration, Y. Sato et al., *Measurement of the lepton forward-backward asymmetry in $B \to X_s \ell^+ \ell^-$ decays with a sum of exclusive modes*, Phys. Rev. **D93** (2016), no. 3 032008, [arXiv:1402.7134]. [Addendum: Phys. Rev.D93,no.5,059901(2016)].

[72] **Belle** Collaboration, D. Dutta et al., *Search for $B_s^0 \to \gamma\gamma$ and a measurement of the branching fraction for $B_s^0 \to \phi\gamma$*, Phys. Rev. **D91** (2015), no. 1 011101, [arXiv:1411.7771].

[73] HFLAV, "$\mathcal{B}(B \to K^*\gamma)$ as of August 2017."
http://www.slac.stanford.edu/xorg/hflav/rare/August2017/radll/index.html.

[74] HLFAV, "A_{CP} as of August 2017."
http://www.slac.stanford.edu/xorg/hflav/rare/August2017/acp/index.html.

[75] HFLAV, "S_{CP} as of Summer 2017." http://www.slac.stanford.edu/xorg/hflav/triangle/summer2017/index.shtml#bsgamma.

[76] **LHCb** Collaboration, R. Aaij et al., *Measurement of the $B_s^0 \to \mu^+\mu^-$ branching fraction and search for $B^0 \to \mu^+\mu^-$ decays at the LHCb experiment*, *Phys. Rev. Lett.* **111** (2013) 101805, [arXiv:1307.5024].

[77] **LHCb** Collaboration, R. Aaij et al., *First experimental study of photon polarization in radiative B_s^0 decays*, *Phys. Rev. Lett.* **118** (2017), no. 2 021801, [arXiv:1609.02032]. [Addendum: Phys. Rev. Lett.118,no.10,109901(2017)].

[78] **LHCb** Collaboration, R. Aaij et al., *Angular analysis of the $B^0 \to K^{*0}e^+e$ decay in the low-q^2 region*, *JHEP* **04** (2015) 064, [arXiv:1501.03038].

[79] **LHCb** Collaboration, R. Aaij et al., *Measurements of the S-wave fraction in $B^0 \to K^+\pi^-\mu^+\mu^-$ decays and the $B^0 \to K^*(892)^0\mu^+\mu^-$ differential branching fraction*, *JHEP* **11** (2016) 047, [arXiv:1606.04731].

A   Additional Figures

In this appendix some additional figures are provided. These use no additional information to those shown in the main text but simply offer a different perspective.
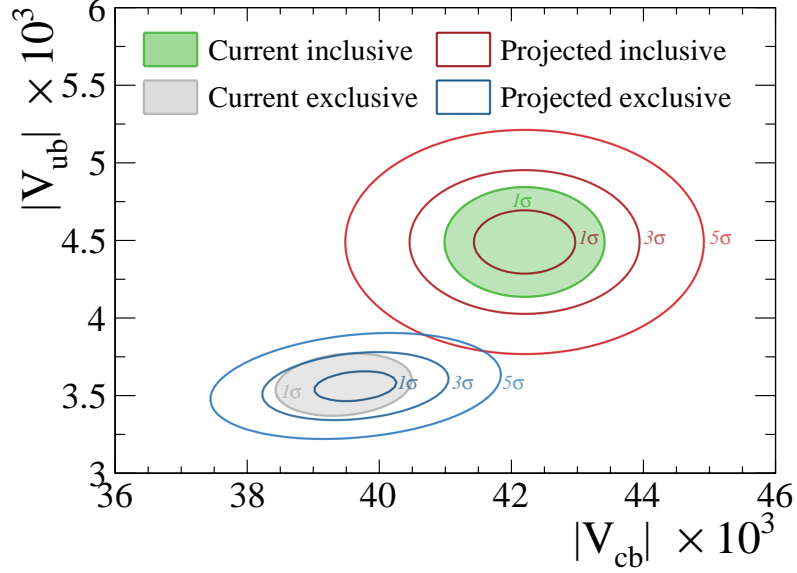
Figure 9: The current (filled areas) and future compatibility, at milestone III, (non-filled areas) of inclusive and exclusive methods for measurements of $|V_{ub}|$ and $|V_{cb}|$
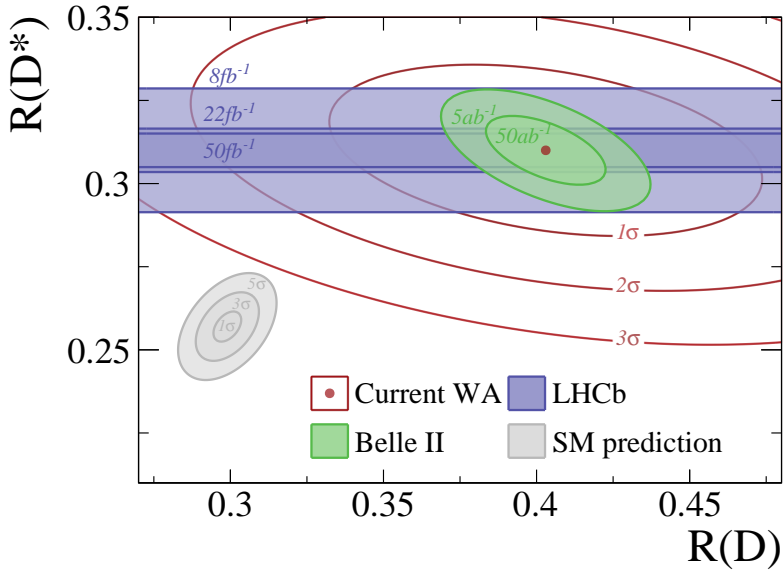
Figure 10: The current world average (red lines), the SM prediction (gray bands) and future prospects from Belle II (green) and LHCb (blue) for measurements of $R(D)$ and $R(D^*)$.
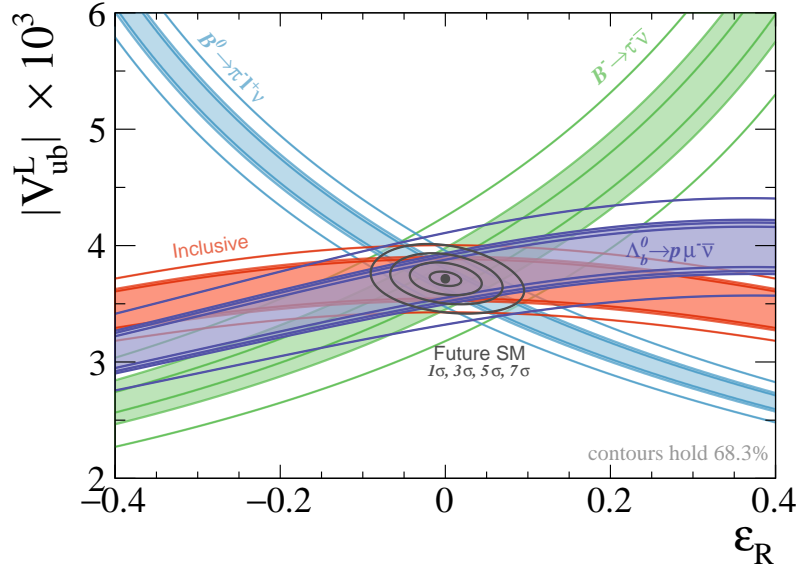
Figure 11: Prospects for new physics measurements related to right handed currents with the central values shifted to the SM expectation. The current uncertainties (not filled) are shown along with the future projections at milestones I, II and III (filled). The SM point (black dot) with the 1σ, 3σ, 5σ and 7σ exclusion contours (black lines) at milestone III are overlaid. Note that changing the central value of $|V_{ub}|$ used in this case simply serves to shift the y-axis.
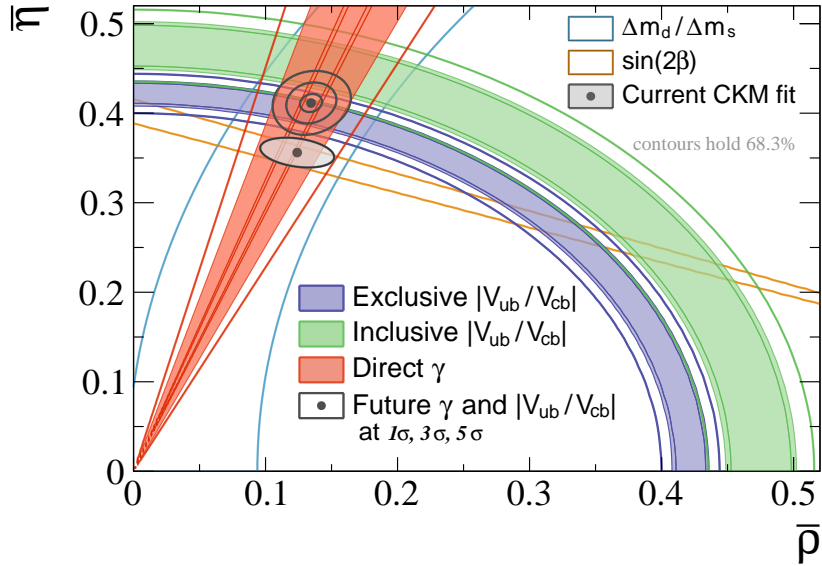
Figure 12: Prospects for CKM fits in $(\bar{\rho}, \bar{\eta})$ space. This is the same plot as shown in Fig. 6 with the current loop-level constraints from $\sin(2\beta)$, Δm_d and Δm_s (values from Ref. [35]) overlaid.

(a) $C_9'^{\mu\mu}$ versus $C_{10}'^{\mu\mu}$.

(b) $\mathcal{R}e\left(C_7'^{\mathrm{NP}}\right)$ versus $\mathcal{I}m\left(C_7'^{\mathrm{NP}}\right)$.
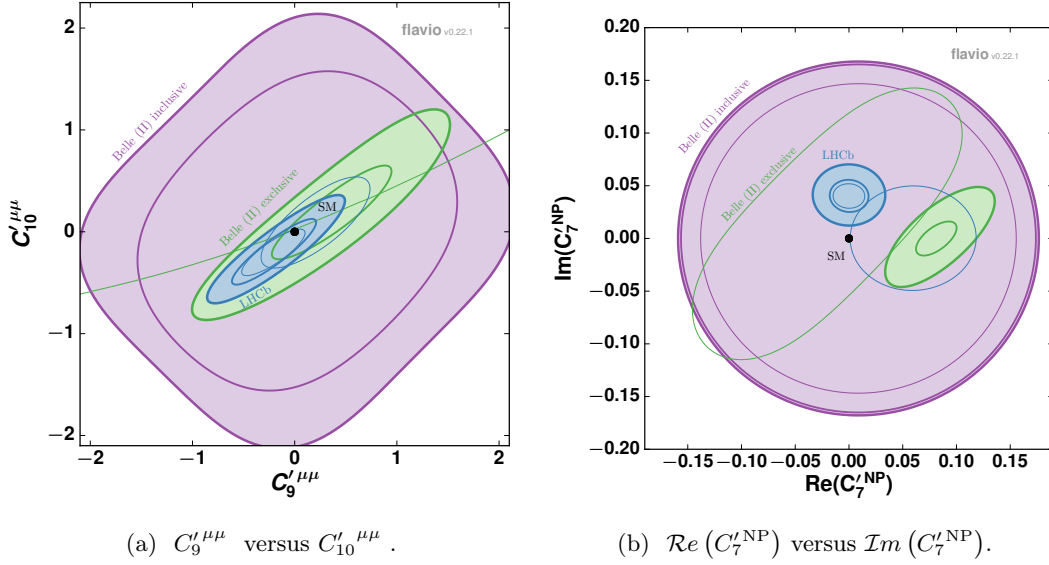
Figure 13: In the two-dimensional scans of pairs of Wilson coefficients, the current average (not filled) as well as the extrapolations to future sensitivities (filled) of LHCb after $8, 22, 50\,\mathrm{fb}^{-1}$ (exclusive) and Belle II after $5, 50\,\mathrm{ab}^{-1}$ (inclusive and exclusive) are given. The central values of the extrapolations have been evaluated in the NP scenarios listed in Table 5. The contours correspond to 1σ uncertainty bands. The Standard Model point (black dot) with the $1\sigma, 3\sigma$, 5σ and 7σ exclusion contours with a combined sensitivity of LHCb's $50\,\mathrm{fb}^{-1}$ and Belle II's $50\,\mathrm{ab}^{-1}$ datasets is indicated in light grey. The primed operators show no tensions with respect to the SM; hence no SM exclusions are provided.

B   Inputs to Wilson coefficient scans

Details on the observables included in the scans of the semi-leptonic and electromagnetic dipole Wilson coefficients are given in Tables tables 7 to 9. The Belle (II) measurements entering the current average and extrapolated sensitivities to $5\,\mathrm{ab}^{-1}$ and $50\,\mathrm{ab}^{-1}$ are summarised in Tables tables 10 to 12, whereas the LHCb measurements are detailed in Tables tables 13 and 14. Corresponding central values as obtained with `flavio` for the SM and various NP models are given in Tables tables 15 to 19. The results of the scans to primed operators are illustrated in Fig. 13.

Table 7: Common inputs for the scans of the semi-leptonic Wilson coefficients. It is indicated if the observable is included in the current average and/or the extrapolations to future milestones.

Observable	q^2 interval	current average	extrapolations
$\mathcal{B}(B \to X_s \mu^+ \mu^-)$	$1.0 < q^2 < 3.5\,\mathrm{GeV}^2$	-	✓
$\mathcal{B}(B \to X_s \mu^+ \mu^-)$	$3.5 < q^2 < 6.0\,\mathrm{GeV}^2$	-	✓
$\mathcal{B}(B \to X_s \mu^+ \mu^-)$	$1.0 < q^2 < 6.0\,\mathrm{GeV}^2$	✓	-
$\mathcal{B}(B \to X_s \mu^+ \mu^-)$	$q^2 > 14.4\,\mathrm{GeV}^2$	✓	✓
$A_{\mathrm{FB}}(B \to X_s \ell^+ \ell^-)$	$1.0 < q^2 < 6.0\,\mathrm{GeV}^2$	✓	-
$A_{\mathrm{FB}}(B \to X_s \ell^+ \ell^-)$	$14.3 < q^2 < 25\,\mathrm{GeV}^2$	✓	-
$A_{\mathrm{FB}}(B \to X_s \ell^+ \ell^-)$	$1.0 < q^2 < 3.5\,\mathrm{GeV}^2$	-	✓
$A_{\mathrm{FB}}(B \to X_s \ell^+ \ell^-)$	$3.5 < q^2 < 6.0\,\mathrm{GeV}^2$	-	✓
$A_{\mathrm{FB}}(B \to X_s \ell^+ \ell^-)$	$q^2 > 14.4\,\mathrm{GeV}^2$	-	✓
$d\mathcal{B}/dq^2(B^+ \to K^+ \mu^+ \mu^-)$	$1.0 < q^2 < 6.0\,\mathrm{GeV}^2$	-	✓
$d\mathcal{B}/dq^2(B^+ \to K^+ \mu^+ \mu^-)$	$1.1 < q^2 < 6.0\,\mathrm{GeV}^2$	✓	✓
$d\mathcal{B}/dq^2(B^+ \to K^+ \mu^+ \mu^-)$	$q^2 > 14.4\,\mathrm{GeV}^2$	-	✓
$d\mathcal{B}/dq^2(B^+ \to K^+ \mu^+ \mu^-)$	$15.0 < q^2 < 22.0\,\mathrm{GeV}^2$	✓	✓
$d\mathcal{B}/dq^2(B^0 \to K^{*0} \mu^+ \mu^-)$	$1.1 < q^2 < 6.0\,\mathrm{GeV}^2$	✓	✓
$d\mathcal{B}/dq^2(B^0 \to K^{*0} \mu^+ \mu^-)$	$15.0 < q^2 < 19.0\,\mathrm{GeV}^2$	✓	✓
$d\mathcal{B}/dq^2(B^0 \to K^{*0} \mu^+ \mu^-)$	$q^2 > 14.4\,\mathrm{GeV}^2$	-	✓
$d\mathcal{B}/dq^2(B_s^0 \to \phi \mu^+ \mu^-)$	$1.0 < q^2 < 6.0\,\mathrm{GeV}^2$	✓	✓
$d\mathcal{B}/dq^2(B_s^0 \to \phi \mu^+ \mu^-)$	$15.0 < q^2 < 19.0\,\mathrm{GeV}^2$	✓	✓
$F_L, A_{\mathrm{FB}}, S_{4,5}(B^0 \to K^{*0} \mu^+ \mu^-)$	$1.1 < q^2 < 2.5\,\mathrm{GeV}^2$	✓	✓
$F_L, A_{\mathrm{FB}}, S_{4,5}(B^0 \to K^{*0} \mu^+ \mu^-)$	$2.5 < q^2 < 4.0\,\mathrm{GeV}^2$	✓	✓
$F_L, A_{\mathrm{FB}}, S_{4,5}(B^0 \to K^{*0} \mu^+ \mu^-)$	$4.0 < q^2 < 6.0\,\mathrm{GeV}^2$	✓	✓
$F_L, A_{\mathrm{FB}}, S_{4,5}(B^0 \to K^{*0} \mu^+ \mu^-)$	$15 < q^2 < 19.0\,\mathrm{GeV}^2$	✓	✓
$P_{4,5}'(B^0 \to K^{*0} \mu^+ \mu^-)$	$0.1 < q^2 < 4.0\,\mathrm{GeV}^2$	✓	-
$P_{4,5}'(B^0 \to K^{*0} \mu^+ \mu^-)$	$1.0 < q^2 < 2.5\,\mathrm{GeV}^2$	-	✓
$P_{4,5}'(B^0 \to K^{*0} \mu^+ \mu^-)$	$2.5 < q^2 < 4.0\,\mathrm{GeV}^2$	-	✓
$P_{4,5}'(B^0 \to K^{*0} \mu^+ \mu^-)$	$4.0 < q^2 < 6.0\,\mathrm{GeV}^2$	-	✓
$P_{4,5}'(B^0 \to K^{*0} \mu^+ \mu^-)$	$14.18 < q^2 < 19.0\,\mathrm{GeV}^2$	✓	✓

Table 8: Specific inputs for the scans of the semi-leptonic Wilson coefficients. It is indicated if the observable is included in the current average and/or the extrapolations to future milestones.

Observable	q^2 interval	current average	extrapolations
Scans including primed coefficients			
$S_3(B^0 \to K^{*0}\mu^+\mu^-)$	$1.1 < q^2 < 2.5\,\text{GeV}^2$	✓	✓
$S_3(B^0 \to K^{*0}\mu^+\mu^-)$	$2.5 < q^2 < 4.0\,\text{GeV}^2$	✓	✓
$S_3(B^0 \to K^{*0}\mu^+\mu^-)$	$4.0 < q^2 < 6.0\,\text{GeV}^2$	✓	✓
$S_3(B^0 \to K^{*0}\mu^+\mu^-)$	$15 < q^2 < 19.0\,\text{GeV}^2$	✓	✓
Scans including $C_{10}^{\text{NP}\,\mu\mu}$			
$\mathcal{B}(B_s \to \mu\mu)$		✓	✓
Scans including electron information			
$P'_{4,5}(B^0 \to K^{*0}e^+e^-)$	$0.1 < q^2 < 4.0\,\text{GeV}^2$	✓	-
$P'_{4,5}(B^0 \to K^{*0}e^+e^-)$	$1.0 < q^2 < 2.5\,\text{GeV}^2$	-	✓
$P'_{4,5}(B^0 \to K^{*0}e^+e^-)$	$2.5 < q^2 < 4.0\,\text{GeV}^2$	-	✓
$P'_{4,5}(B^0 \to K^{*0}e^+e^-)$	$4.0 < q^2 < 6.0\,\text{GeV}^2$	-	✓
$P'_{4,5}(B^0 \to K^{*0}e^+e^-)$	$14.18 < q^2 < 19.0\,\text{GeV}^2$	✓	✓
$R(X_s)$	$1.0 < q^2 < 6.0\,\text{GeV}^2$	✓	✓
$R(X_s)$	$q^2 > 14.4\,\text{GeV}^2$	✓	✓
$R(K)$	$1.0 < q^2 < 6.0\,\text{GeV}^2$	✓	✓
$R(K)$	$q^2 > 14.4\,\text{GeV}^2$	-	✓
$R(K)$	$15.0 < q^2 < 22.0\,\text{GeV}^2$	-	✓
$R(K^*)$	$0.045 < q^2 < 1.1\,\text{GeV}^2$	✓	✓
$R(K^*)$	$1.1 < q^2 < 6.0\,\text{GeV}^2$	✓	✓
$R(K^*)$	$15.0 < q^2 < 19.0\,\text{GeV}^2$	-	✓
$R(K^*)$	$q^2 > 14.4\,\text{GeV}^2$	-	✓
$R(\phi)$	$1.0 < q^2 < 6.0\,\text{GeV}^2$	-	✓
$R(\phi)$	$15.0 < q^2 < 19.0\,\text{GeV}^2$	-	✓

Table 9: Inputs for the scans of the electromagnetic dipole Wilson coefficients. It is indicated if the observable is included in the current average and/or the extrapolations to future milestones.

Observable	q^2 interval	current average	extrapolations
$\mathcal{B}(B_s^0 \to \phi\gamma)$		✓	✓
$\mathcal{B}(B^+ \to K^{*+}\gamma)$		✓	✓
$\mathcal{A}^{CP}(B^+ \to K^{*+}\gamma)$		✓	✓
$\mathcal{B}(B^0 \to K^{*0}\gamma)$		✓	✓
$\mathcal{A}^{CP}(B^0 \to K^{*0}\gamma)$		✓	✓
$\mathcal{B}(B \to X_s\gamma)$		✓	✓
$A^{\Delta\Gamma}(B_s^0 \to \phi\gamma)$		✓	✓
$S_{K^*\gamma}$		✓	✓
$P_1(B^0 \to K^{*0}e^+e^-)$	$0.002 < q^2 < 1.12\,\mathrm{GeV}^2$	✓	✓
$A_T^{\mathrm{Im}}(B^0 \to K^{*0}e^+e^-)$	$0.002 < q^2 < 1.12\,\mathrm{GeV}^2$	✓	✓
$A_{7,8,9}(B^0 \to K^{*0}\mu^+\mu^-)$	$1.1 < q^2 < 2.5\,\mathrm{GeV}^2$	✓	✓
$A_{7,8,9}(B^0 \to K^{*0}\mu^+\mu^-)$	$2.5 < q^2 < 4.0\,\mathrm{GeV}^2$	✓	✓
$A_{7,8,9}(B^0 \to K^{*0}\mu^+\mu^-)$	$4.0 < q^2 < 6.0\,\mathrm{GeV}^2$	✓	✓
$A_{8,9}(B^0 \to K^{*0}\mu^+\mu^-)$	$15 < q^2 < 19.0\,\mathrm{GeV}^2$	✓	✓

Table 10: Summary of inclusive inputs for the current measurement and extrapolations of the Belle (II) inclusive measurements. For the published measurements, the appropriate reference is given. The extrapolated uncertainties comprise statistical and systematic uncertainties.

Observable	q^2 interval	Measurement $0.7\,\mathrm{ab}^{-1}$	Extrapolations $5\,\mathrm{ab}^{-1}$	$50\,\mathrm{ab}^{-1}$
$\mathcal{B}(B \to X_s\gamma)$		$(3.06 \pm 0.11 \pm 0.24 \pm 0.09) \times 10^{-4}$ [69]	3.9%	3.2%
$\mathcal{B}(B \to X_s\mu^+\mu^-)$	$1.0 < q^2 < 3.5\,\mathrm{GeV}^2$	-	17%	7.4%
$\mathcal{B}(B \to X_s\mu^+\mu^-)$	$3.5 < q^2 < 6.0\,\mathrm{GeV}^2$	-	14%	6.8%
$\mathcal{B}(B \to X_s\mu^+\mu^-)$	$1.0 < q^2 < 6.0\,\mathrm{GeV}^2$	$(0.66^{+0.82}_{-0.76}\,{}^{+0.30}_{-0.24} \pm 0.07) \times 10^{-6}$ [70]	-	-
$\mathcal{B}(B \to X_s\mu^+\mu^-)$	$q^2 > 14.4\,\mathrm{GeV}^2$	$(0.60^{+0.31}_{-0.29}\,{}^{+0.05}_{-0.04}) \times 10^{-6}$ [70]	12%	5.1%
$A_{\mathrm{FB}}(B \to X_s\ell^+\ell^-)$	$1.0 < q^2 < 6.0\,\mathrm{GeV}^2$	$0.30 \pm 0.24 \pm 0.04$ [71]	-	-
$A_{\mathrm{FB}}(B \to X_s\ell^+\ell^-)$	$14.3 < q^2 < 25.0\,\mathrm{GeV}^2$	$0.28 \pm 0.15 \pm 0.02$ [71]	-	-
$A_{\mathrm{FB}}(B \to X_s\ell^+\ell^-)$	$1.0 < q^2 < 3.5\,\mathrm{GeV}^2$	-	15%	4.7%
$A_{\mathrm{FB}}(B \to X_s\ell^+\ell^-)$	$3.5 < q^2 < 6.0\,\mathrm{GeV}^2$	-	12%	3.8%
$A_{\mathrm{FB}}(B \to X_s\ell^+\ell^-)$	$q^2 > 14.4\,\mathrm{GeV}^2$	-	9.5%	3.1%
$R(X_s)$	$1.0 < q^2 < 6.0\,\mathrm{GeV}^2$	0.34 ± 0.43 [70][vi]	12%	4%
$R(X_s)$	$q^2 > 14.4\,\mathrm{GeV}^2$	1.07 ± 0.64 [70][vi]	17%	5.3%

[vi] Calculated from Table I assuming fully correlated model and systematic uncertainties.

Table 11: Summary of exclusive inputs for the current measurement and extrapolations of the Belle (II) exclusive measurements. For the published measurements, the appropriate reference is given. The extrapolated uncertainties comprise statistical and systematic uncertainties.

Observable	q^2 interval	Measurement $0.7\,\mathrm{ab}^{-1}$	Extrapolations	
			$5\,\mathrm{ab}^{-1}$	$50\,\mathrm{ab}^{-1}$
$\mathcal{B}(B_s^0 \to \phi\gamma)$		$(3.6 \pm 0.5 \pm 0.3 \pm 0.6) \times 10^{-5}$ [72]	-	-
$\mathcal{B}(B^+ \to K^{*+}\gamma)$		$(39.2^{+1.3}_{-1.2}) \times 10^{-6}$ [73]	1.8×10^{-6}	1.8×10^{-6}
$\mathcal{A}^{CP}(B^+ \to K^{*+}\gamma)$		0.012 ± 0.023 [74]	0.0081	0.0029
$\mathcal{B}(B^0 \to K^{*0}\gamma)$		$(41.8 \pm 1.2) \times 10^{-6}$ [73]	1.5×10^{-6}	1.5×10^{-6}
$\mathcal{A}^{CP}(B^0 \to K^{*0}\gamma)$		-0.007 ± 0.011 [74]	0.0058	0.0021
$S_{K^*\gamma}$		-0.16 ± 0.22 [75]	0.09	0.03
$A_T^{(2)}(B^0 \to K^{*0}e^+e^-)$	$0.002 < q^2 < 1.12\,\mathrm{GeV}^2$	-	0.21	0.066
$A_T^{\mathrm{Im}}(B^0 \to K^{*0}e^+e^-)$	$0.002 < q^2 < 1.12\,\mathrm{GeV}^2$	-	0.20	0.064
$R(K)$	$1.0 < q^2 < 6.0\,\mathrm{GeV}^2$	-	11%	3.6%
$R(K)$	$q^2 > 14.4\,\mathrm{GeV}^2$	-	12%	3.6%
$R(K^*)$	$1.1 < q^2 < 6.0\,\mathrm{GeV}^2$	-	10%	3.2%
$R(K^*)$	$q^2 > 14.4\,\mathrm{GeV}^2$	-	9.2%	2.8%
$d\mathcal{B}/dq^2(B^+ \to K^+\mu^+\mu^-)$	$1.0 < q^2 < 6.0\,\mathrm{GeV}^2$	-	10%	4%
$d\mathcal{B}/dq^2(B^+ \to K^+\mu^+\mu^-)$	$q^2 > 14.4\,\mathrm{GeV}^2$	-	10%	4%
$d\mathcal{B}/dq^2(B^0 \to K^{*0}\mu^+\mu^-)$	$1.1 < q^2 < 6.0\,\mathrm{GeV}^2$	-	10%	4%
$d\mathcal{B}/dq^2(B^0 \to K^{*0}\mu^+\mu^-)$	$q^2 > 14.4\,\mathrm{GeV}^2$	-	10%	4%

Table 12: Summary of exclusive inputs for the current measurement and extrapolations of the Belle (II) exclusive measurements. For the published measurements, the appropriate reference is given. The extrapolated uncertainties comprise statistical and systematic uncertainties.

Observable	q^2 interval	Measurement $0.7\,\mathrm{ab}^{-1}$	Extrapolations	
			$5\,\mathrm{ab}^{-1}$	$50\,\mathrm{ab}^{-1}$
$P_4'(B^0 \to K^{*0}\mu^+\mu^-)$	$0.1 < q^2 < 4.0\,\mathrm{GeV}^2$	$-0.38^{+0.50}_{-0.48} \pm 0.12$ [22]	-	-
$P_4'(B^0 \to K^{*0}\mu^+\mu^-)$	$1.0 < q^2 < 2.5\,\mathrm{GeV}^2$	-	0.27	0.08
$P_4'(B^0 \to K^{*0}\mu^+\mu^-)$	$2.5 < q^2 < 4.0\,\mathrm{GeV}^2$	-	0.24	0.08
$P_4'(B^0 \to K^{*0}\mu^+\mu^-)$	$4.0 < q^2 < 6.0\,\mathrm{GeV}^2$	-	0.19	0.06
$P_4'(B^0 \to K^{*0}\mu^+\mu^-)$	$14.18 < q^2 < 19.0\,\mathrm{GeV}^2$	$-0.10^{+0.39}_{-0.39} \pm 0.07$ [22]	0.13	0.04
$P_5'(B^0 \to K^{*0}\mu^+\mu^-)$	$0.1 < q^2 < 4.0\,\mathrm{GeV}^2$	$0.42^{+0.39}_{-0.39} \pm 0.14$ [22]	-	-
$P_5'(B^0 \to K^{*0}\mu^+\mu^-)$	$1.0 < q^2 < 2.5\,\mathrm{GeV}^2$	-	0.25	0.08
$P_5'(B^0 \to K^{*0}\mu^+\mu^-)$	$2.5 < q^2 < 4.0\,\mathrm{GeV}^2$	-	0.23	0.07
$P_5'(B^0 \to K^{*0}\mu^+\mu^-)$	$4.0 < q^2 < 6.0\,\mathrm{GeV}^2$	-	0.18	0.06
$P_5'(B^0 \to K^{*0}\mu^+\mu^-)$	$14.18 < q^2 < 19.0\,\mathrm{GeV}^2$	$-0.13^{+0.39}_{-0.35} \pm 0.06$ [22]	0.11	0.04
$P_4'(B^0 \to K^{*0}e^+e^-)$	$0.1 < q^2 < 4.0\,\mathrm{GeV}^2$	$0.34^{+0.41}_{-0.45} \pm 0.11$ [22]	-	-
$P_4'(B^0 \to K^{*0}e^+e^-)$	$1.0 < q^2 < 2.5\,\mathrm{GeV}^2$	-	0.24	0.07
$P_4'(B^0 \to K^{*0}e^+e^-)$	$2.5 < q^2 < 4.0\,\mathrm{GeV}^2$	-	0.22	0.07
$P_4'(B^0 \to K^{*0}e^+e^-)$	$4.0 < q^2 < 6.0\,\mathrm{GeV}^2$	-	0.18	0.06
$P_4'(B^0 \to K^{*0}e^+e^-)$	$14.18 < q^2 < 19.0\,\mathrm{GeV}^2$	$-0.15^{+0.41}_{-0.40} \pm 0.04$ [22]	0.16	0.05
$P_5'(B^0 \to K^{*0}e^+e^-)$	$0.1 < q^2 < 4.0\,\mathrm{GeV}^2$	$0.51^{+0.39}_{-0.46} \pm 0.09$ [22]	-	-
$P_5'(B^0 \to K^{*0}e^+e^-)$	$1.0 < q^2 < 2.5\,\mathrm{GeV}^2$	-	0.23	0.07
$P_5'(B^0 \to K^{*0}e^+e^-)$	$2.5 < q^2 < 4.0\,\mathrm{GeV}^2$	-	0.21	0.07
$P_5'(B^0 \to K^{*0}e^+e^-)$	$4.0 < q^2 < 6.0\,\mathrm{GeV}^2$	-	0.17	0.06
$P_5'(B^0 \to K^{*0}e^+e^-)$	$14.18 < q^2 < 19.0\,\mathrm{GeV}^2$	$-0.91^{+0.36}_{-0.30} \pm 0.03$ [22]	0.14	0.04

Table 13: Summary of inputs for the current measurement and extrapolations of the LHCb measurements. For the published measurements, the appropriate reference is given. The extrapolated uncertainties comprise solely statistical uncertainties.

Observable	q^2 interval	Measurement $3\,\mathrm{fb}^{-1}$	Extrapolations		
			$8\,\mathrm{fb}^{-1}$	$22\,\mathrm{fb}^{-1}$	$50\,\mathrm{fb}^{-1}$
$\mathcal{B}(B_s^0 \to \mu^+\mu^-)$		$(2.9^{+1.1}_{-1.0}{}^{+0.3}_{-0.1}) \times 10^{-9}$ [76][vii]	0.44×10^{-9}	0.24×10^{-9}	0.16×10^{-9}
$\mathcal{B}(B_s^0 \to \phi\gamma)$		$(3.5 \pm 0.3) \times 10^{-5}$ [50][viii]	0.3×10^{-5}	0.3×10^{-5}	0.3×10^{-5}
$\mathcal{A}^{\Delta\Gamma}(B_s^0 \to \phi\gamma)$		$-0.98^{+0.46}_{-0.52}{}^{+0.23}_{-0.20}$ [77]	0.27	0.11	0.07
$A_T^{(2)}(B^0 \to K^{*0}e^+e^-)$	$0.002 < q^2 < 1.12\,\mathrm{GeV}^2$	$-0.23 \pm 0.23 \pm 0.05$ [78]	0.120	0.053	0.033
$A_T^{\mathrm{Im}}(B^0 \to K^{*0}e^+e^-)$	$0.002 < q^2 < 1.12\,\mathrm{GeV}^2$	$0.14 \pm 0.22 \pm 0.05$ [78]	0.115	0.050	0.032
$R(\phi)$	$1.0 < q^2 < 6.0\,\mathrm{GeV}^2$	-	0.159	0.086	0.056
$R(\phi)$	$15.0 < q^2 < 19.0\,\mathrm{GeV}^2$	-	0.137	0.074	0.048
$R(K)$	$1.0 < q^2 < 6.0\,\mathrm{GeV}^2$	$0.745^{+0.090}_{-0.074} \pm 0.036$ [17]	0.046	0.025	0.016
$R(K)$	$15.0 < q^2 < 22.0\,\mathrm{GeV}^2$	-	0.043	0.023	0.015
$R(K^*)$	$0.045 < q^2 < 1.1\,\mathrm{GeV}^2$	$0.66^{+0.11}_{-0.07} \pm 0.03$ [18]	0.048	0.026	0.017
$R(K^*)$	$1.1 < q^2 < 6.0\,\mathrm{GeV}^2$	$0.69^{+0.11}_{-0.07} \pm 0.05$ [18]	0.053	0.028	0.019
$R(K^*)$	$15.0 < q^2 < 19.0\,\mathrm{GeV}^2$	-	0.061	0.033	0.021
$d\mathcal{B}/dq^2(B^+ \to K^+\mu^+\mu^-)$	$1.1 < q^2 < 6.0\,\mathrm{GeV}^2$	$(24.2 \pm 0.7 \pm 1.2) \times 10^{-9}$ [19]	0.7×10^{-9}	0.4×10^{-9}	0.3×10^{-9}
$d\mathcal{B}/dq^2(B^+ \to K^+\mu^+\mu^-)$	$15.0 < q^2 < 22.0\,\mathrm{GeV}^2$	$(12.1 \pm 0.4 \pm 0.6) \times 10^{-9}$ [19]	0.4×10^{-9}	0.2×10^{-9}	0.1×10^{-9}
$d\mathcal{B}/dq^2(B^0 \to K^{*0}\mu^+\mu^-)$	$1.1 < q^2 < 6.0\,\mathrm{GeV}^2$	$(0.342^{+0.017}_{-0.017} \pm 0.009 \pm 0.023) \times 10^{-7}$ [79]	0.015×10^{-7}	0.008×10^{-7}	0.005×10^{-7}
$d\mathcal{B}/dq^2(B^0 \to K^{*0}\mu^+\mu^-)$	$15.0 < q^2 < 19.0\,\mathrm{GeV}^2$	$(0.436^{+0.018}_{-0.019} \pm 0.007 \pm 0.030) \times 10^{-7}$ [79]	0.018×10^{-7}	0.010×10^{-7}	0.006×10^{-7}
$d\mathcal{B}/dq^2(B_s^0 \to \phi\mu^+\mu^-)$	$1.0 < q^2 < 6.0\,\mathrm{GeV}^2$	$(2.58^{+0.33}_{-0.31} \pm 0.08 \pm 0.19) \times 10^{-8}$ [23]	0.20×10^{-8}	0.11×10^{-8}	0.07×10^{-8}
$d\mathcal{B}/dq^2(B_s^0 \to \phi\mu^+\mu^-)$	$15.0 < q^2 < 19.0\,\mathrm{GeV}^2$	$(4.04^{+0.39}_{-0.38} \pm 0.13 \pm 0.30) \times 10^{-8}$ [23]	0.26×10^{-8}	0.14×10^{-8}	0.09×10^{-8}

[vii] The extrapolations of the LHCb measurement of $B_s^0 \to \mu^+\mu^-$ do not rely on the quoted measured branching fraction on the $3\,\mathrm{fb}^{-1}$ dataset of Run 1 [76] but on the update including partial data from Run 2 on $4.4\,\mathrm{fb}^{-1}$ [59].

[viii] This measurement has been performed on $1\,\mathrm{fb}^{-1}$ and has been extrapolated to $3\,\mathrm{fb}^{-1}$ under the assumption that the uncertainty arising from f_s/f_d is irreducible

Table 14: Summary of inputs for the current measurement and extrapolations of the LHCb measurements. For the published measurements, the appropriate reference is given. The extrapolated uncertainties comprise solely statistical uncertainties.

Observable	q^2 interval	Measurement	Extrapolations		
		$3\,\mathrm{fb}^{-1}$	$8\,\mathrm{fb}^{-1}$	$22\,\mathrm{fb}^{-1}$	$50\,\mathrm{fb}^{-1}$
$S_3(B^0 \to K^{*0}\mu^+\mu^-)$	$1.1 < q^2 < 2.5\,\mathrm{GeV}^2$	$-0.077^{+0.087}_{-0.105} \pm 0.005$ [21]	0.049	0.027	0.017
$S_4(B^0 \to K^{*0}\mu^+\mu^-)$	$1.1 < q^2 < 2.5\,\mathrm{GeV}^2$	$-0.077^{+0.111}_{-0.113} \pm 0.005$ [21]	0.057	0.031	0.020
$S_5(B^0 \to K^{*0}\mu^+\mu^-)$	$1.1 < q^2 < 2.5\,\mathrm{GeV}^2$	$0.137^{+0.099}_{-0.094} \pm 0.009$ [21]	0.050	0.027	0.018
$F_L(B^0 \to K^{*0}\mu^+\mu^-)$	$1.1 < q^2 < 2.5\,\mathrm{GeV}^2$	$0.660^{+0.083}_{-0.077} \pm 0.022$ [21]	0.042	0.023	0.015
$A_{\mathrm{FB}}(B^0 \to K^{*0}\mu^+\mu^-)$	$1.1 < q^2 < 2.5\,\mathrm{GeV}^2$	$-0.191^{+0.068}_{-0.080} \pm 0.012$ [21]	0.038	0.021	0.014
$A_7(B^0 \to K^{*0}\mu^+\mu^-)$	$1.1 < q^2 < 2.5\,\mathrm{GeV}^2$	$-0.087^{+0.091}_{-0.093} \pm 0.004$ [21]	0.047	0.025	0.017
$A_8(B^0 \to K^{*0}\mu^+\mu^-)$	$1.1 < q^2 < 2.5\,\mathrm{GeV}^2$	$-0.044^{+0.108}_{-0.113} \pm 0.005$ [21]	0.057	0.031	0.020
$A_9(B^0 \to K^{*0}\mu^+\mu^-)$	$1.1 < q^2 < 2.5\,\mathrm{GeV}^2$	$-0.004^{+0.092}_{-0.098} \pm 0.005$ [21]	0.049	0.026	0.017
$S_3(B^0 \to K^{*0}\mu^+\mu^-)$	$2.5 < q^2 < 4.0\,\mathrm{GeV}^2$	$0.035^{+0.098}_{-0.089} \pm 0.007$ [21]	0.048	0.026	0.017
$S_4(B^0 \to K^{*0}\mu^+\mu^-)$	$2.5 < q^2 < 4.0\,\mathrm{GeV}^2$	$-0.234^{+0.127}_{-0.144} \pm 0.006$ [21]	0.070	0.038	0.025
$S_5(B^0 \to K^{*0}\mu^+\mu^-)$	$2.5 < q^2 < 4.0\,\mathrm{GeV}^2$	$-0.022^{+0.110}_{-0.103} \pm 0.008$ [21]	0.055	0.030	0.019
$F_L(B^0 \to K^{*0}\mu^+\mu^-)$	$2.5 < q^2 < 4.0\,\mathrm{GeV}^2$	$0.876^{+0.109}_{-0.097} \pm 0.017$ [21]	0.053	0.029	0.019
$A_{\mathrm{FB}}(B^0 \to K^{*0}\mu^+\mu^-)$	$2.5 < q^2 < 4.0\,\mathrm{GeV}^2$	$-0.118^{+0.082}_{-0.090} \pm 0.007$ [21]	0.044	0.024	0.016
$A_7(B^0 \to K^{*0}\mu^+\mu^-)$	$2.5 < q^2 < 4.0\,\mathrm{GeV}^2$	$-0.032^{+0.109}_{-0.115} \pm 0.005$ [21]	0.057	0.031	0.020
$A_8(B^0 \to K^{*0}\mu^+\mu^-)$	$2.5 < q^2 < 4.0\,\mathrm{GeV}^2$	$-0.071^{+0.124}_{-0.131} \pm 0.006$ [21]	0.065	0.035	0.023
$A_9(B^0 \to K^{*0}\mu^+\mu^-)$	$2.5 < q^2 < 4.0\,\mathrm{GeV}^2$	$-0.228^{+0.114}_{-0.152} \pm 0.007$ [21]	0.068	0.037	0.024
$S_3(B^0 \to K^{*0}\mu^+\mu^-)$	$4.0 < q^2 < 6.0\,\mathrm{GeV}^2$	$0.035^{+0.069}_{-0.068} \pm 0.007$ [21]	0.035	0.019	0.012
$S_4(B^0 \to K^{*0}\mu^+\mu^-)$	$4.0 < q^2 < 6.0\,\mathrm{GeV}^2$	$-0.219^{+0.086}_{-0.084} \pm 0.008$ [21]	0.044	0.024	0.015
$S_5(B^0 \to K^{*0}\mu^+\mu^-)$	$4.0 < q^2 < 6.0\,\mathrm{GeV}^2$	$-0.146^{+0.077}_{-0.078} \pm 0.011$ [21]	0.040	0.022	0.014
$F_L(B^0 \to K^{*0}\mu^+\mu^-)$	$4.0 < q^2 < 6.0\,\mathrm{GeV}^2$	$0.611^{+0.052}_{-0.053} \pm 0.017$ [21]	0.028	0.015	0.010
$A_{\mathrm{FB}}(B^0 \to K^{*0}\mu^+\mu^-)$	$4.0 < q^2 < 6.0\,\mathrm{GeV}^2$	$0.025^{+0.051}_{-0.052} \pm 0.004$ [21]	0.027	0.014	0.009
$A_7(B^0 \to K^{*0}\mu^+\mu^-)$	$4.0 < q^2 < 6.0\,\mathrm{GeV}^2$	$0.041^{+0.083}_{-0.082} \pm 0.004$ [21]	0.042	0.023	0.015
$A_8(B^0 \to K^{*0}\mu^+\mu^-)$	$4.0 < q^2 < 6.0\,\mathrm{GeV}^2$	$0.004^{+0.093}_{-0.095} \pm 0.005$ [21]	0.048	0.026	0.017
$A_9(B^0 \to K^{*0}\mu^+\mu^-)$	$4.0 < q^2 < 6.0\,\mathrm{GeV}^2$	$0.062^{+0.078}_{-0.072} \pm 0.004$ [21]	0.038	0.021	0.014
$S_3(B^0 \to K^{*0}\mu^+\mu^-)$	$15 < q^2 < 19.0\,\mathrm{GeV}^2$	$-0.163^{+0.033}_{-0.033} \pm 0.009$ [21]	0.017	0.009	0.006
$S_4(B^0 \to K^{*0}\mu^+\mu^-)$	$15 < q^2 < 19.0\,\mathrm{GeV}^2$	$-0.284^{+0.038}_{-0.041} \pm 0.007$ [21]	0.021	0.011	0.007
$S_5(B^0 \to K^{*0}\mu^+\mu^-)$	$15 < q^2 < 19.0\,\mathrm{GeV}^2$	$-0.325^{+0.036}_{-0.037} \pm 0.009$ [21]	0.019	0.011	0.007
$F_L(B^0 \to K^{*0}\mu^+\mu^-)$	$15.0 < q^2 < 19.0\,\mathrm{GeV}^2$	$0.344^{+0.028}_{-0.030} \pm 0.008$ [21]	0.015	0.008	0.005
$A_{\mathrm{FB}}(B^0 \to K^{*0}\mu^+\mu^-)$	$15.0 < q^2 < 19.0\,\mathrm{GeV}^2$	$0.355^{+0.027}_{-0.027} \pm 0.009$ [21]	0.015	0.008	0.005
$A_8(B^0 \to K^{*0}\mu^+\mu^-)$	$15.0 < q^2 < 19.0\,\mathrm{GeV}^2$	$0.025^{+0.048}_{-0.047} \pm 0.003$ [21]	0.025	0.013	0.009
$A_9(B^0 \to K^{*0}\mu^+\mu^-)$	$15.0 < q^2 < 19.0\,\mathrm{GeV}^2$	$0.061^{+0.043}_{-0.044} \pm 0.002$ [21]	0.023	0.012	0.008

Table 15: Summary of the Belle (II) inclusive measurements and the corresponding central values for the SM and the different NP scenarios as obtained with the `flavio` package.

Observable	q^2 interval	SM	$(C_9^{\text{NP}\mu\mu}, C_{10}^{\text{NP}\mu\mu})$ $(-0.8, 0.6)$	$(C_9'^{\mu\mu}, C_{10}'^{\mu\mu})$ $(0.8, 0.2)$	$(C_9^{\text{NP}\mu\mu}, C_9^{\text{NP}ee})$ $(-0.8, 0.4)$	$(\mathcal{R}e\,(C_7^{\text{NP}}), \mathcal{I}m\,(C_7^{\text{NP}}))$ $(0.02, -0.06)$	$(\mathcal{R}e\,(C_7'^{\text{NP}}), \mathcal{I}m\,(C_7'^{\text{NP}}))$ $(-0.050, -0.075)$
$\mathcal{B}(B\to X_s\gamma)\,[10^{-4}]$		3.30	-	-		3.36	4.14
$\mathcal{B}(B\to X_s\mu^+\mu^-)\,[10^{-6}]$	$1.0 < q^2 < 3.5\,\text{GeV}^2$	0.92	0.67	0.94	0.81	-	-
$\mathcal{B}(B\to X_s\mu^+\mu^-)\,[10^{-6}]$	$3.5 < q^2 < 6.0\,\text{GeV}^2$	0.76	0.52	0.77	0.64	-	-
$\mathcal{B}(B\to X_s\mu^+\mu^-)\,[10^{-6}]$	$q^2 > 14.4\,\text{GeV}^2$	0.31	0.22	0.32	0.27	-	-
$A_{\text{FB}}(B\to X_s\ell^+\ell^-)$	$1.0 < q^2 < 3.5\,\text{GeV}^2$	-0.080	-0.098	-0.079	-0.088	-	-
$A_{\text{FB}}(B\to X_s\ell^+\ell^-)$	$3.5 < q^2 < 6.0\,\text{GeV}^2$	0.065	0.047	0.066	0.055	-	-
$A_{\text{FB}}(B\to X_s\ell^+\ell^-)$	$q^2 > 14.4\,\text{GeV}^2$	-0.066	-0.061	-0.063	-0.062	-	-
$R(X_s)$	$1.0 < q^2 < 6.0\,\text{GeV}^2$	0.963	-	-	0.772	-	-
$R(X_s)$	$q^2 > 14.4\,\text{GeV}^2$	1.149	-	-	0.923	-	-

Table 16: Summary of the Belle (II) exclusive measurements and the corresponding central values for the SM and the different NP scenarios as obtained with the `flavio` package.

Observable	q^2 interval	SM	$(C_9^{\mathrm{NP}\mu\mu}, C_{10}^{\mathrm{NP}\mu\mu})$ $(-1.4, 0.4)$	$(C_9'^{\mu\mu}, C_{10}'^{\mu\mu})$ $(0.4, 0.2)$	$(C_9^{\mathrm{NP}\mu\mu}, C_9^{\mathrm{NP}ee})$ $(-1.4, -0.7)$	$(\mathcal{R}e\,(C_7'^{\mathrm{NP}}), \mathcal{I}m\,(C_7'^{\mathrm{NP}}))$ $(0.08, 0.00)$	$(\mathcal{R}e\,(C_7^{\mathrm{NP}}), \mathcal{I}m\,(C_7^{\mathrm{NP}}))$ $(-0.050, 0.050)$
$\mathcal{B}(B^+ \to K^{*+}\gamma)\,[10^{-6}]$		41.8	-	-	-	43.5	54.6
$\mathcal{A}^{CP}(B^+ \to K^{*+}\gamma)$		0.0053	-	-	-	0.0051	-0.0114
$\mathcal{B}(B^0 \to K^{*0}\gamma)\,[10^{-6}]$		42.1	-	-	-	43.6	54.5
$\mathcal{A}^{CP}(B^0 \to K^{*0}\gamma)$		0.0036	-	-	-	0.0034	-0.0116
$S_{K^*\gamma}$		-0.02	-	-	-	0.27	-0.02
$A_T^{(2)}(B^0 \to K^{*0}e^+e^-)$	$0.002 < q^2 < 1.12\,\mathrm{GeV}^2$	0.037	-	-	-	-0.379	0.032
$A_T^{\mathrm{Im}}(B^0 \to K^{*0}e^+e^-)$	$0.002 < q^2 < 1.12\,\mathrm{GeV}^2$	0.000	-	-	-	-0.003	0.004
$R(K)$	$1.0 < q^2 < 6.0\,\mathrm{GeV}^2$	1.000	-	-	0.857	-	-
$R(K)$	$q^2 > 14.4\,\mathrm{GeV}^2$	1.003	-	-	0.861	-	-
$R(K^*)$	$1.1 < q^2 < 6.0\,\mathrm{GeV}^2$	0.996	-	-	0.908	-	-
$R(K^*)$	$q^2 > 14.4\,\mathrm{GeV}^2$	0.998	-	-	0.861	-	-
$d\mathcal{B}/dq^2(B^+ \to K^+\mu^+\mu^-)\,[10^{-9}]$	$1.0 < q^2 < 6.0\,\mathrm{GeV}^2$	36.5	23.0	38.3	26.5	-	-
$d\mathcal{B}/dq^2(B^+ \to K^+\mu^+\mu^-)\,[10^{-9}]$	$q^2 > 14.4\,\mathrm{GeV}^2$	11.9	7.5	12.5	8.7	-	-
$d\mathcal{B}/dq^2(B^0 \to K^{*0}\mu^+\mu^-)\,[10^{-7}]$	$1.1 < q^2 < 6.0\,\mathrm{GeV}^2$	0.475	0.334	0.467	0.387	-	-
$d\mathcal{B}/dq^2(B^0 \to K^{*0}\mu^+\mu^-)\,[10^{-7}]$	$q^2 > 14.4\,\mathrm{GeV}^2$	0.272	0.172	0.265	0.200	-	-

Table 17: Summary of the Belle (II) exclusive measurements and the corresponding central values for the SM and the different NP scenarios as obtained with the `flavio` package.

Observable	q^2 interval	SM	$(C_9^{\mathrm{NP}\mu\mu}, C_{10}^{\mathrm{NP}\mu\mu})$ $(-1.4, 0.4)$	$(C_9'^{\mu\mu}, C_{10}'^{\mu\mu})$ $(0.4, 0.2)$	$(C_9^{\mathrm{NP}\mu\mu}, C_9^{\mathrm{NP}ee})$ $(-1.4, -0.7)$	$(\mathcal{Re}(C_7^{\mathrm{NP}}), \mathcal{Im}(C_7^{\mathrm{NP}}))$ $(0.08, 0.00)$	$(\mathcal{Re}(C_7'^{\mathrm{NP}}), \mathcal{Im}(C_7'^{\mathrm{NP}}))$ $(-0.050, 0.050)$
$P_4'(B^0 \to K^{*0}\mu^+\mu^-)$	$1.0 < q^2 < 2.5\,\mathrm{GeV}^2$	-0.04	-0.04	-0.07	-0.08	-	-
$P_4'(B^0 \to K^{*0}\mu^+\mu^-)$	$2.5 < q^2 < 4.0\,\mathrm{GeV}^2$	-0.39	-0.32	-0.41	-0.35	-	-
$P_4'(B^0 \to K^{*0}\mu^+\mu^-)$	$4.0 < q^2 < 6.0\,\mathrm{GeV}^2$	-0.50	-0.47	-0.51	-0.48	-	-
$P_4'(B^0 \to K^{*0}\mu^+\mu^-)$	$14.18 < q^2 < 19.0\,\mathrm{GeV}^2$	-0.63	-0.63	-0.62	-0.63	-	-
$P_5'(B^0 \to K^{*0}\mu^+\mu^-)$	$1.0 < q^2 < 2.5\,\mathrm{GeV}^2$	-0.17	0.49	0.21	0.48	-	-
$P_5'(B^0 \to K^{*0}\mu^+\mu^-)$	$2.5 < q^2 < 4.0\,\mathrm{GeV}^2$	-0.50	-0.04	-0.48	-0.04	-	-
$P_5'(B^0 \to K^{*0}\mu^+\mu^-)$	$4.0 < q^2 < 6.0\,\mathrm{GeV}^2$	-0.76	-0.43	-0.75	-0.40	-	-
$P_5'(B^0 \to K^{*0}\mu^+\mu^-)$	$14.18 < q^2 < 19.0\,\mathrm{GeV}^2$	-0.62	-0.55	-0.64	-0.52	-	-
$P_4'(B^0 \to K^{*0}e^+e^-)$	$1.0 < q^2 < 2.5\,\mathrm{GeV}^2$	-0.04	-	-	-0.05	-	-
$P_4'(B^0 \to K^{*0}e^+e^-)$	$2.5 < q^2 < 4.0\,\mathrm{GeV}^2$	-0.39	-	-	-0.37	-	-
$P_4'(B^0 \to K^{*0}e^+e^-)$	$4.0 < q^2 < 6.0\,\mathrm{GeV}^2$	-0.50	-	-	-0.49	-	-
$P_4'(B^0 \to K^{*0}e^+e^-)$	$14.18 < q^2 < 19.0\,\mathrm{GeV}^2$	-0.63	-	-	-0.63	-	-
$P_5'(B^0 \to K^{*0}e^+e^-)$	$1.0 < q^2 < 2.5\,\mathrm{GeV}^2$	0.17	-	-	0.32	-	-
$P_5'(B^0 \to K^{*0}e^+e^-)$	$2.5 < q^2 < 4.0\,\mathrm{GeV}^2$	-0.50	-	-	-0.28	-	-
$P_5'(B^0 \to K^{*0}e^+e^-)$	$4.0 < q^2 < 6.0\,\mathrm{GeV}^2$	-0.75	-	-	-0.61	-	-
$P_5'(B^0 \to K^{*0}e^+e^-)$	$14.18 < q^2 < 19.0\,\mathrm{GeV}^2$	-0.62	-	-	-0.59	-	-

Table 18: Summary of the LHCb measurements and the corresponding central values for the SM and the different NP scenarios as obtained with the flavio package.

Observable	q^2 interval	SM	$(C_9^{\mathrm{NP}\,\mu\mu}, C_{10}^{\mathrm{NP}\,\mu\mu})$ $(-1.0, 0.0)$	$(C_9'^{\,\mu\mu}, C_{10}'^{\,\mu\mu})$ $(-0.2, -0.2)$	$(C_9^{\mathrm{NP}\,\mu\mu}, C_9^{\mathrm{NP}\,ee})$ $(-1.0, 0.0)$	$(\mathcal{Re}(C_7^{\mathrm{NP}}), \mathcal{Im}(C_7^{\mathrm{NP}}))$ $(0.00, 0.04)$	$(\mathcal{Re}(C_7'^{\mathrm{NP}}), \mathcal{Im}(C_7'^{\mathrm{NP}}))$ $(-0.075, 0.000)$
$\mathcal{B}(B_s^0 \to \mu^+\mu^-)$ [10^{-9}]		3.60	3.60	3.27	-	-	-
$\mathcal{B}(B_s^0 \to \phi\gamma)$ [10^{-5}]		4.1	-	-	-	4.1	5.8
$A^{\Delta\Gamma}(B_s^0 \to \phi\gamma)$		0.03	-	-	-	0.03	0.03
$A_T^{(2)}(B^0 \to K^{*0}e^+e^-)$	$0.002 < q^2 < 1.12\,\mathrm{GeV}^2$	0.037	-	-	-	0.038	0.033
$A_T^{\mathrm{Im}}(B^0 \to K^{*0}e^+e^-)$	$0.002 < q^2 < 1.12\,\mathrm{GeV}^2$	0.000	-	-	-	-0.213	0.032
$R(\phi)$	$1.0 < q^2 < 6.0\,\mathrm{GeV}^2$	0.997	-	-	0.840	-	-
$R(\phi)$	$15.0 < q^2 < 19.0\,\mathrm{GeV}^2$	0.998	-	-	0.795	-	-
$R(K)$	$1.0 < q^2 < 6.0\,\mathrm{GeV}^2$	1.000	-	-	0.793	-	-
$R(K)$	$15.0 < q^2 < 22.0\,\mathrm{GeV}^2$	1.003	-	-	0.797	-	-
$R(K^*)$	$0.045 < q^2 < 1.1\,\mathrm{GeV}^2$	0.945	-	-	0.911	-	-
$R(K^*)$	$1.1 < q^2 < 6.0\,\mathrm{GeV}^2$	0.996	-	-	0.846	-	-
$R(K^*)$	$15.0 < q^2 < 19.0\,\mathrm{GeV}^2$	0.998	-	-	0.796	-	-
$d\mathcal{B}/dq^2(B^+ \to K^+\mu^+\mu^-)$ [10^{-9}]	$1.1 < q^2 < 6.0\,\mathrm{GeV}^2$	36.5	28.9	36.7	28.9	-	-
$d\mathcal{B}/dq^2(B^+ \to K^+\mu^+\mu^-)$ [10^{-9}]	$15.0 < q^2 < 22.0\,\mathrm{GeV}^2$	15.6	12.4	15.6	12.4	-	-
$d\mathcal{B}/dq^2(B^0 \to K^{*0}\mu^+\mu^-)$ [10^{-7}]	$1.1 < q^2 < 6.0\,\mathrm{GeV}^2$	0.475	0.407	0.477	0.407	-	-
$d\mathcal{B}/dq^2(B^0 \to K^{*0}\mu^+\mu^-)$ [10^{-7}]	$15.0 < q^2 < 19.0\,\mathrm{GeV}^2$	0.596	0.475	0.594	0.475	-	-
$d\mathcal{B}/dq^2(B_s^0 \to \phi\mu^+\mu^-)$ [10^{-8}]	$1.0 < q^2 < 6.0\,\mathrm{GeV}^2$	5.38	4.54	5.37	4.54	-	-
$d\mathcal{B}/dq^2(B_s^0 \to \phi\mu^+\mu^-)$ [10^{-8}]	$15.0 < q^2 < 19.0\,\mathrm{GeV}^2$	5.56	4.43	5.55	4.43	-	-

Table 19: Summary of the LHCb measurements and the corresponding central values for the SM and the different NP scenarios as obtained with the flavio package.

Observable	q^2 interval	SM	$(C_9^{\mathrm{NP}\mu\mu}, C_{10}^{\mathrm{NP}\mu\mu})$ $(-1.0, 0.0)$	$(C_9^{\prime\,\mu\mu}, C_{10}^{\prime\,\mu\mu})$ $(-0.2, -0.2)$	$(C_9^{\mathrm{NP}\mu\mu}, C_9^{\mathrm{NP}ee})$ $(-1.0, 0.0)$	$(\mathcal{R}e(C_7^{\prime\,\mathrm{NP}}), \mathcal{I}m(C_7^{\prime\,\mathrm{NP}}))$ $(0.00, 0.04)$	$(\mathcal{R}e(C_7^{\mathrm{NP}}), \mathcal{I}m(C_7^{\mathrm{NP}}))$ $(-0.075, 0.000)$
$S_3(B^0 \to K^{*0}\mu^+\mu^-)$	$1.1 < q^2 < 2.5\,\mathrm{GeV}^2$	0.002	-	0.011	-	-	-
$S_4(B^0 \to K^{*0}\mu^+\mu^-)$	$1.1 < q^2 < 2.5\,\mathrm{GeV}^2$	−0.026	−0.034	−0.015	−0.034	-	-
$S_5(B^0 \to K^{*0}\mu^+\mu^-)$	$1.1 < q^2 < 2.5\,\mathrm{GeV}^2$	0.056	0.164	0.035	0.164	-	-
$F_L(B^0 \to K^{*0}\mu^+\mu^-)$	$1.1 < q^2 < 2.5\,\mathrm{GeV}^2$	0.760	0.682	0.760	0.682	-	-
$A_{\mathrm{FB}}(B^0 \to K^{*0}\mu^+\mu^-)$	$1.1 < q^2 < 2.5\,\mathrm{GeV}^2$	−0.137	−0.192	−0.136	−0.192	-	-
$A_7(B^0 \to K^{*0}\mu^+\mu^-)$	$1.1 < q^2 < 2.5\,\mathrm{GeV}^2$	0.003	-	-	-	−0.037	0.003
$A_8(B^0 \to K^{*0}\mu^+\mu^-)$	$1.1 < q^2 < 2.5\,\mathrm{GeV}^2$	0.001	-	-	-	0.018	0.001
$A_9(B^0 \to K^{*0}\mu^+\mu^-)$	$1.1 < q^2 < 2.5\,\mathrm{GeV}^2$	0.000	-	-	-	−0.021	0.000
$S_3(B^0 \to K^{*0}\mu^+\mu^-)$	$2.5 < q^2 < 4.0\,\mathrm{GeV}^2$	−0.011	-	−0.002	-	-	-
$S_4(B^0 \to K^{*0}\mu^+\mu^-)$	$2.5 < q^2 < 4.0\,\mathrm{GeV}^2$	−0.152	−0.150	−0.144	−0.150	-	-
$S_5(B^0 \to K^{*0}\mu^+\mu^-)$	$2.5 < q^2 < 4.0\,\mathrm{GeV}^2$	−0.192	−0.077	−0.207	−0.077	-	-
$F_L(B^0 \to K^{*0}\mu^+\mu^-)$	$2.5 < q^2 < 4.0\,\mathrm{GeV}^2$	0.796	0.747	0.797	0.747	-	-
$A_{\mathrm{FB}}(B^0 \to K^{*0}\mu^+\mu^-)$	$2.5 < q^2 < 4.0\,\mathrm{GeV}^2$	−0.016	−0.096	−0.016	−0.096	-	-
$A_7(B^0 \to K^{*0}\mu^+\mu^-)$	$2.5 < q^2 < 4.0\,\mathrm{GeV}^2$	0.002	-	-	-	−0.026	0.002
$A_8(B^0 \to K^{*0}\mu^+\mu^-)$	$2.5 < q^2 < 4.0\,\mathrm{GeV}^2$	0.001	-	-	-	0.015	0.001
$A_9(B^0 \to K^{*0}\mu^+\mu^-)$	$2.5 < q^2 < 4.0\,\mathrm{GeV}^2$	0.000	-	-	-	−0.002	0.000
$S_3(B^0 \to K^{*0}\mu^+\mu^-)$	$4.0 < q^2 < 6.0\,\mathrm{GeV}^2$	−0.025	-	−0.017	-	-	-
$S_4(B^0 \to K^{*0}\mu^+\mu^-)$	$4.0 < q^2 < 6.0\,\mathrm{GeV}^2$	−0.225	−0.221	−0.219	−0.221	-	-
$S_5(B^0 \to K^{*0}\mu^+\mu^-)$	$4.0 < q^2 < 6.0\,\mathrm{GeV}^2$	−0.337	−0.240	−0.347	−0.240	-	-
$F_L(B^0 \to K^{*0}\mu^+\mu^-)$	$4.0 < q^2 < 6.0\,\mathrm{GeV}^2$	0.709	0.687	0.713	0.687	-	-
$A_{\mathrm{FB}}(B^0 \to K^{*0}\mu^+\mu^-)$	$4.0 < q^2 < 6.0\,\mathrm{GeV}^2$	0.125	0.041	0.123	0.041	-	-
$A_7(B^0 \to K^{*0}\mu^+\mu^-)$	$4.0 < q^2 < 6.0\,\mathrm{GeV}^2$	0.002	-	-	-	−0.017	0.002
$A_8(B^0 \to K^{*0}\mu^+\mu^-)$	$4.0 < q^2 < 6.0\,\mathrm{GeV}^2$	0.001	-	-	-	0.012	0.001
$A_9(B^0 \to K^{*0}\mu^+\mu^-)$	$4.0 < q^2 < 6.0\,\mathrm{GeV}^2$	0.000	-	-	-	0.006	0.000
$S_3(B^0 \to K^{*0}\mu^+\mu^-)$	$15.0 < q^2 < 19.0\,\mathrm{GeV}^2$	−0.204	-	−0.203	-	-	-
$S_4(B^0 \to K^{*0}\mu^+\mu^-)$	$15 < q^2 < 19.0\,\mathrm{GeV}^2$	−0.301	−0.301	−0.301	−0.301	-	-
$S_5(B^0 \to K^{*0}\mu^+\mu^-)$	$15 < q^2 < 19.0\,\mathrm{GeV}^2$	−0.281	−0.255	−0.283	−0.255	-	-
$F_L(B^0 \to K^{*0}\mu^+\mu^-)$	$15.0 < q^2 < 19.0\,\mathrm{GeV}^2$	0.343	0.343	0.343	0.343	-	-
$A_{\mathrm{FB}}(B^0 \to K^{*0}\mu^+\mu^-)$	$15.0 < q^2 < 19.0\,\mathrm{GeV}^2$	0.366	0.329	0.368	0.329	-	-
$A_8(B^0 \to K^{*0}\mu^+\mu^-)$	$15.0 < q^2 < 19.0\,\mathrm{GeV}^2$	0.000	-	-	-	0.003	0.000
$A_9(B^0 \to K^{*0}\mu^+\mu^-)$	$15.0 < q^2 < 19.0\,\mathrm{GeV}^2$	0.000	-	-	-	0.006	0.000